01 Aug 1996

Behavior of compression web members in cold-formed steel truss assemblies

Jerome A. Riemann

Roger A. LaBoube
Missouri University of Science and Technology, laboube@mst.edu

Wei-Wen Yu
Missouri University of Science and Technology, wwy4@mst.edu

Civil Engineering Study 96-1
Cold-Formed Steel Series

Second Summary Report

BEHAVIOR OF COMPRESSION WEB MEMBERS IN COLD-FORMED STEEL TRUSS ASSEMBLIES

by

Jerome A. Riemann
Research Assistant

Roger A. LaBoube
Wei-Wen Yu
Project Directors

A Research Project Sponsored by
National Science Foundation
Grant No. MSS-9222022
and
American Iron and Steel Institute

August 1996

Department of Civil Engineering
Center for Cold-Formed Steel Structures
University of Missouri-Rolla
Rolla, Missouri

PREFACE

To aid in adapting cold-formed steel to the residential market, a research project was initiated in 1993 at the University of Missouri-Rolla. Design issues relating to the use of cold-formed steel members and connections in residential roof truss systems have been the focus of the project. The purpose of this research was to study the behavior of cold-formed steel roof truss systems and to establish appropriate design recommendations. Overall, the research findings were intended to aid the promotion of cold-formed steel as a safe, serviceable, and cost effective alternative in residential construction.

The First Summary Report was issued in May 1995. The report outlined the research effort to date which included a review of available literature, followed by a comparative analysis of experimental truss behavior to a computer generated model. The experimental investigation involved an evaluation of the overall truss behavior using full-scale truss assemblies. Based on this information, a computer generated model was created to simulate the truss assembly. An evaluation of deflection and stress data was used to correlate the computer model to the full-scale truss. The computer model and AISI Specification formed the basis used to establish the predicted failure load, which was then compared to the tested failure of the full-scale truss assembly. The conclusions obtained from the experimental investigation were used to formulate design recommendations.

This second summary report focuses on the behavior of the web members of a cold-formed steel truss assembly. Twenty-eight full-scale tests were completed in this phase of the study. The truss assemblies were fabricated using C-sections with top chords continuous from heel-to-ridge, bottom chord continuous from heel-to-heel, and web members

connecting between the chords. All connections were made using 3/4 in. long, No. 10, self-drilling screws. The pitch of the top chord was maintained at 4:12 for all truss assemblies. The compression web members had thicknesses from 0.0360 to 0.0593 in. Web members had slenderness ratios that varied from 100 to 180. The data recorded consisted of measurements of transverse deflections at the midspan of the compression web member, strain measurements at the same location, and the end reactions at the truss supports. Recommendations are made for the modeling of truss assemblies and the design of compression web members.

This report is based on the thesis presented to the Faculty of the Graduate School of the University of Missouri-Rolla in partial fulfillment of the requirements for the degree of Masters of Science in Civil Engineering.

This material is based upon work supported by the National Science Foundation under Grant No. MSS-9222022 and by the American Iron and Steel Institute. The technical guidance provided by the Technological Research Subcommittee of the AISI Residential Advisory Committee is gratefully acknowledged. Thanks are also extended to A. Ziolkowski and R. B. Haws, AISI staff, and J. B. Scalzi of the National Science Foundation. Any opinions, findings, and conclusions or recommendations expressed in this material are those of the authors and do not reflect the views of the National Science Foundation.

TABLE OF CONTENTS

Page

Page

LIST OF ILLUSTRATIONS

LIST OF TABLES

I. INTRODUCTION

A. GENERAL

Traditionally wood has been the primary material used in the framing of residential construction; however, cold-formed steel has begun to replace wood as a residential construction material in many areas of the country. Cold-formed steel members are structural shapes that are formed from sheet steel without an elevation of temperature. Although cold-formed sections have just begun to be widely used in residential construction, they have been used for many years in commercial buildings, automobiles, storage racks, and other manufactured products to provide economical and serviceable designs.

There are many advantages in replacing wooden studs, joists, and trusses with their cold-formed steel counterparts. A primary reason driving the change to steel products is economics. Haynes and Fight[1], research foresters with the Forestry Sciences Laboratory, project that a reduction in the supply of high quality lumber will result in the prices continuing to rise. The reduction in the supply of high quality lumber is due in part to concerns that the lumber industry is depleting the nations forest lands. Substituting steel for lumber in the framing of residential construction will help ease the demand on the Nation's forest lands.

In addition to economic and environmental concerns, the high strength-to-weight ratio of steel makes it an economical replacement for lumber in residential construction. The consistent high quality of steel products makes steel a serviceable building material

in that steel sections do not split or warp as often occurs with lumber. Steel sections also eliminate the concerns of combustibility and termite damage.

To enable the most efficient and cost effective design of cold-formed steel roof trusses, an investigation was began in 1994 at the University of Missouri-Rolla to address design considerations concerning the use of cold-formed steel truss assemblies in residential roofing applications. This phase of the study has focused on the compression web members of the truss assemblies.

B. PURPOSE OF INVESTIGATION

The purpose of this investigation is to develop design recommendations for the use of cold-formed steel truss assemblies in residential roofing applications. An understanding of the behavior of cold-formed steel trusses must be achieved in order to develop recommendations for their design. The intent of the University of Missouri-Rolla studies is to perform experimental work as necessary to develop such an understanding of the behavior. Previous University of Missouri-Rolla research focused on the behavior of the chord member and the appropriate analytical modeling assumptions. This phase of the study has focused on the compression web members within the truss assemblies.

C. SCOPE OF INVESTIGATION

This study is the continuation of work performed by Harper[2] which focused on the overall behavior and top chord of the truss assemblies. This phase of the investigation focused on the compression web members of the truss assemblies. Full

scale tests were performed to study the behavior of the compression web members in cold-formed steel roof trusses subjected to uniformly distributed gravity load. The trusses were fabricated using C-sections with a top chord member continuous from heel-to-peak, a bottom chord member continuous from heel-to-heel, and web members connecting between the chords. All connections were made with 3/4 inch, No. 10, self-drilling screws. The geometry of the truss assembly is discussed in detail in Section III-C. The pitch of the top chord was maintained at 4:12 for all truss assemblies. The thickness of the compression web members studied varied from 0.0360 inches to 0.0593 inches. The ratio of the length to the radius of gyration, (L/r), of the compression web members was varied from 100 to 180.

The data recorded consisted of measurements of transverse deflections at the midspan of the compression web member, strain measurements at the same location, and the end reactions at the supports of the truss assembly.

II. LITERATURE SEARCH

A. GENERAL

The configuration and load application of a truss results in members that may act in flexure, compression, tension, a combination of flexure and compression, or a combination of flexure and tension. The following discussion focuses on the behavior and design of cold-formed steel members and connections as related to their application in floor or roof trusses.

B. TENSION MEMBERS

In gravity loaded floor and roof trusses, the bottom chord and certain web members may be subjected to pure tension. The design capacity of an axially loaded tension member is controlled by yielding of the net cross section. As described in Section C2 of the AISI Specification[3], the allowable capacity of a tension member is given by T_a as follows:

$$T_a = \frac{T_n}{\Omega_t} \qquad (1)$$

where $T_n = A_n F_y$, Nominal strength of member loaded in tension

$\Omega_t = 1.67$, Factor of safely for tension

A_n = Net area of the cross section

F_y = Yield point of the tension member

C. FLEXURAL MEMBERS

In truss assemblies typically used in residential construction some of the individual members may be subjected to bending as a result of the applied loading. Other members in the truss assemblies could also be subjected to bending as a result of eccentricities in the connections of the members. Flexural members are used to resist bending moments caused by the applied loading. As described by Yu[4], the design of flexural members must consider the moment resisting capacity of the section while checking the web for shear, combined bending and shear, web crippling, and combined bending and web crippling. Attention should also be given to the lateral buckling strength of the section. As described in section C3 of the AISI Specification[3], the bending moment applied to flexural members should not exceed the allowable bending capacity, M_a, as follows:

$$M_a = \frac{M_n}{\Omega_f} \qquad (2)$$

where M_n = Smaller of the nominal bending capacities for the nominal section strength and the lateral buckling strength

Ω_f = 1.67, Factor of safety for flexure

As discussed in the specification, the effective element design widths should be used to compute the section properties when applicable. As discussed in section C3.1.1, the effective section modulus for nominal section strength should be calculated with the extreme compression or tension fiber at the yield point, F_y. Likewise, in section C3.1.2, AISI requires that the effective section modulus for lateral buckling strength be calculated

with the extreme compression fiber at the stress produced by the critical lateral buckling moment. Section B2 requires that the effective moment of inertia used to compute deflections be based upon the stress level that is produced in the exterior fibers as a result of the applied service loads.

D. COMPRESSION MEMBERS

For floor and roof truss assemblies subjected to a downward gravity load, the top chord and certain web members will act in axial compression or a combination of axial compression and bending.

1. Axially Loaded. As discussed by Yu[4], the possible failure modes for axially loaded compression members are 1) yielding, 2) overall column buckling, and 3) local buckling of the elements. Only short, compact compression members will fail in yielding; therefore, overall buckling is the predominate mode of failure in axially loaded compression members. There are three possible modes of overall column buckling: flexural, torsional, and torsional-flexural. Concentrically loaded compression members must be designed in accordance with Section C4 of the AISI Specification[3] such that the axial load shall not exceed the allowable axial load, P_a. The allowable axial load is calculated as follows:

$$P_a = \frac{P_n}{\Omega_c} \qquad (3)$$

where $P_n = A_e F_n$, Nominal axial strength

A_e = Effective area at the stress F_n

F_n = Critical stress as determined in AISI Sections C4.1 through C4.3.

Ω_c = Factor of Safety for axial compression

1.92, except when the controlling behavior is inelastic buckling, the section is fully effective, and the thickness is greater than or equal to 0.09 inches. In this case, Ω_c must be calculated according to the special provisions described in Section C4 of the AISI Specification[3].

AISI recognizes the effects of local buckling by reducing the effective area of the cross-section as described in section B2.2a of the AISI Specification.

2. Beam-Columns. Beam-columns are members which are subjected to axial compression and bending. Due to the nature of structural systems most columns are subjected to bending caused by eccentric loading, transverse loading, geometrical imperfections, or moments applied through end conditions. Section C5 of the AISI Specification[3] requires that the axial force and bending moments in beam-columns should meet the following conditions.

$$\frac{P}{P_a}+\frac{C_{mx}M_x}{M_{ax}\alpha_x}+\frac{C_{my}M_y}{M_{ay}\alpha_y}\leq 1.0 \qquad (4)$$

$$\frac{P}{P_{ao}}+\frac{M_x}{M_{ax}}+\frac{M_y}{M_{ay}}\leq 1.0 \qquad (5)$$

where P = Applied axial load

P_{ao} = Allowable axial load for a column based upon the limit state of yielding

M_{ax} & M_{ay} = Allowable moments about the centroidal axes

$1/\alpha_x$ & $1/\alpha_y$ = $1/[1-(\Omega_c P/P_{cr})]$, Magnification factors

P_{cr} = Elastic buckling strength about axis of bending

C_{mx} & C_{my} = End moment coefficients for x & y axes

Equation 4, which is equation C5-1 in the AISI Specification[3], is used to check stability of the beam-column away from the ends of the member. The magnification factors, $1/\alpha$, account for the second order effects caused by transverse deflections in beam-columns. Equation 5, which is AISI equation C5-2, is used to check yielding at the ends of the member.

3. End Conditions. The end restraint conditions for compression members are recognized through the use of an effective length factor, K, which is a ratio of the effective column length to the actual unbraced length. For design purposes the effective length, KL, of a column is adjusted to reflect the connections restraint to rotation and translation.

As discussed by Salmon & Johnson[5], and Galambos[6], end restraint against rotation and translation may be present in web members of trusses. Consequently, K could be taken as less than unity. Since trusses designed for moving live load, do not simultaneously develop maximum stresses in adjacent members, K may be taken as 0.85. However, statically loaded trusses that are optimally designed develop maximum stresses in all members at approximately the same time. Since adjacent members near maximum

stress levels can not provide adequate rotational or translational restraint, K should be taken as unity for web members in statically loaded trusses.

In the Standard Specifications for Longspan Steel Joists and Deep Longspan Steel Joists[7] issued by the Steel Joist Institute, requirements are given for the design of compression web members. Compression web members in these series of steel joists are typically double angle members connected to the chord members by welds. If the double angles are connected between panel points with fillers or ties, the double angles will act as a single built-up member. Otherwise, the double angles will act individually as single component members. In either case, the Steel Joist Institute allows K to be taken as 0.75 for in-plane bending. However, K must be taken as unity for out-of-plane bending.

4. Transverse Deflections. Melcher[8] discusses the problem of transverse deflections in axially loaded "real" columns with geometrical imperfections. In a study of columns with initial out-of-straightness, it was found that the magnitude and direction of the initial deflection influences the buckling characteristics and buckling strength of singly symmetrical sections. Recognizing that these deflections can affect the buckling strength of the columns, Melcher contends that the ultimate load carrying capacity is a matter of not just the ultimate strength, but also the corresponding deflections. A design approach is presented which derives the ultimate design load by placing a limit on the transverse deflection. This deflection limitation at the ultimate load carrying capacity of columns is different from the serviceability limit states in that excessive transverse deflections in columns can cause unacceptable changes in the system geometry. Melcher notes that the ultimate deflection concept is also significant in the case of eccentrically loaded beam-columns.

E. CONNECTIONS

The method of connecting individual members is a critical part of the construction of cold-formed steel trusses. The AISI Specification[3] states that connections should be designed to transmit the maximum load that the connected member must carry. The specification further states that eccentricities should be considered in the design. The specification only contains design requirements for welded, bolted, and screwed connections. The AISI specification provisions for screwed connections were issued in a Center for Cold-Formed Steel Structures Technical Bulletin[9].

Research has been performed by Pedreschi and Sinha[10] at the University of Edinburgh, Scotland regarding the application of press-joining as a method of connecting cold-formed steel truss members. Press-joining is a relatively new method of connecting steel sheet by a shearing and deformation action. The press joint method of connections is currently being used in the United States in the fabrication of cold-formed steel trusses.

F. TRUSS RESEARCH

Ife[11] studied a research house constructed with cold-formed steel members. The design of the roofing trusses was based on a study of three truss configurations. The first truss studied was a standard "W" truss made with cold-formed C-sections and connections were made by gusset plates and spot welds. The first truss failed at approximately half the predicted failure load due to failure of the welds. The premature failure was believed to have been caused by high connection stresses resulting from the eccentricities in the connections. The second truss was the same configuration as the first except that connections were made with self-drilling screws. The screw connections

were found to perform better than the welds; however, failure of the connections still occurred before the predicted failure load was reached. A third truss was constructed with hat sections for chord members and mechanical tubing for web members. This configuration removed the eccentricities in the connections and the predicted failure load was reached. The third truss configuration was used as a model for the actual trusses in the research house.

Woolcock and Kitipornchai[12] proposed a design method for single angle web struts in trusses. The design method was based upon experimental observations in which the dominate mode of deformation was perpendicular to the plane of the truss. This direction of deformation did not coincide with the principal axes. It was believed that the influence of the end restraint caused the deformation to occur perpendicular to the plane of the truss instead of about the principal axes as would be expected. Since it was observed that the end restraint caused the deformations to occur perpendicular to the plane of the truss, it was reasoned that only flexural buckling perpendicular to the plane of the truss must be considered. The design method recommended accounting for the eccentric loading by applying equal and opposite, out of plane, end moments.

The current study at the University of Missouri-Rolla is an extension of work performed by Harper[2]. Harper's study involved developing a computer analysis model, and conducting full-scale tests of 20 ft. span Fink truss assemblies having a 4:12 top chord pitch. The truss assemblies were fabricated using cold-formed steel C-sections and self-drilling screws. Two identical trusses were positioned side by side 24 inches apart and covered with 48 inch wide plywood sheathing. To provide the lateral stability that an entire roofing system would provide, lateral braces were provided to prevent lateral

buckling of the entire truss assembly. Common masonry bricks were placed on the sheathing to provide the gravity loading. Harper concluded that for top chord members that are continuous from heel to ridge, the effective length factor, K, could be taken as 0.75. However, the web members were observed to act essentially as pin-ended compression members. Consequently, K was taken as 1.0 for web members in cold-formed steel truss assemblies.

The Design Guide for Cold-Formed Steel Trusses[13] gives the following recommendation for the design of compression web members in cold-formed steel trusses.

> For a web member connected to the web of the chord members, or connected to gusset plates, the axial compression load may be taken as acting through the centroid of the web member's cross-section.
>
> The design strength may be determined using Section C4 of the Specification (1986). When computing the design strength, the unbraced lengths, L_x, L_y, and L_t, may be taken as the distance between the center of the member's end connection patterns. The effective length factor K may be taken as unity.

III. EXPERIMENTAL STUDY

A. GENERAL

A study of the behavior of cold-formed steel trusses as used in residential roofing applications was began at the University of Missouri-Rolla in 1994. The purpose of the study is to gain an understanding of the behavior of cold-formed steel trusses to aid in the development of design recommendations. The initial phase of the University of Missouri-Rolla research performed by Harper[2] addressed the overall behavior of the cold-formed steel truss assemblies, with particular attention given to the ultimate capacity of the top chord. The current phase of the study has focused on the behavior and design considerations of the compression web members within the truss assembly. Cold-formed steel C-sections and self-drilling screws were used to construct all the trusses studied in this study. The first series of tests in this phase of the study was performed at the Mitek Inc. research and development facility in St. Louis, MO during June and July 1995. The second series of tests was performed at the University of Missouri-Rolla Engineering Research Laboratory during February and March 1996.

B. TEST SPECIMENS

All of the truss assemblies studied in this experimental program were constructed using cold-formed steel C-sections and self-drilling screws. The nominal depth of the C-sections varied from 2.5 inches to 8 inches. All of the flanges were edge-stiffened and had a width of approximately 1 5/8 inches. The mechanical properties of each C-section were determined by performing tensile tests on coupons cut from the web of the sections.

The actual measured dimensions and material properties of each C-section are shown in Table I and the dimensions are defined in Figure 1.

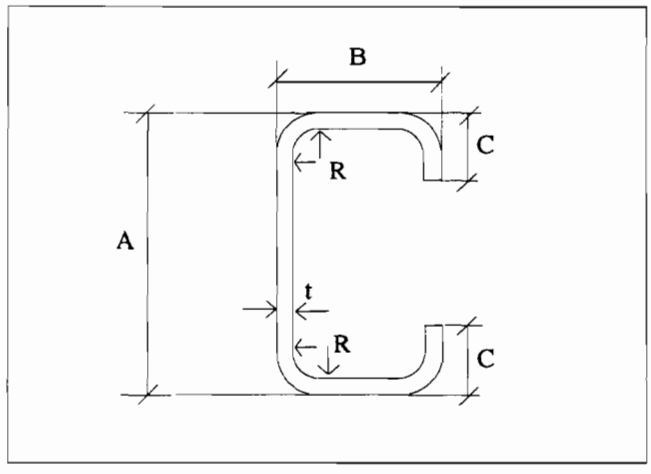

Figure 1. Definition of Cross-Sectional Dimensions

Table I. WEB MEMBER DIMENSIONS AND MECHANICAL PROPERTIES

SECTION	DIMENSIONS (INCHES)					MECHANICAL PROPERTIES		
	A	B	C	t	R	Fy (ksi)	Fu (ksi)	% Elongation
TYPE I	2.5	1.56	0.375	0.0469	0.156	42.5	56.4	39.7
TYPE II	2.5	1.56	0.375	0.0593	0.156	38.3	50.5	49.6
TYPE III	2.5	1.56	0.563	0.0360	0.156	31.0	46.6	53.1
TYPE IV	2.5	1.56	0.563	0.0457	0.156	52.5	59.3	39.4
TYPE V	2.5	1.56	0.563	0.0551	0.156	60.5	72.1	36.2

C. TRUSS ASSEMBLY

The truss assemblies were designed such that the compression web member would be the weakest structural element. This insured that the behavior of the web member could be investigated to failure before the other elements in the truss failed. The parameters believed to significantly affect the behavior of the compression web members were slenderness ratio, end fixity, and thickness. Therefore, these parameters were investigated in the experimental study.

Detailed drawings of the truss assemblies used in each test are contained in Appendix A. These drawings provide the overall dimensions of the truss assemblies and the nominal sizes of each individual member.

1. First Series of Tests. Single slope truss assemblies were fabricated using cold-formed steel C-sections and self-drilling screws. The assembled trusses were transported to the Mitek, Inc. research and development facility in St. Louis, Missouri where full-scale testing was conducted. The truss assemblies were fabricated consistent with typical residential construction practices and the previous University of Missouri-Rolla work of Harper[2]. All trusses were constructed with the top chord at a 4:12 pitch. The basic test assembly is shown in Figure 2.

The heel connection was fabricated by coping the top flange of the bottom chord; this facilitated the top chord nesting inside the bottom chord. With this type of connection, the top and bottom chord C-sections could face the same direction. Additional screws were placed in the heel connection such that the web of the bottom chord would remain in contact with the web of the top chord. Figure 3 shows the configuration of the heel connection.

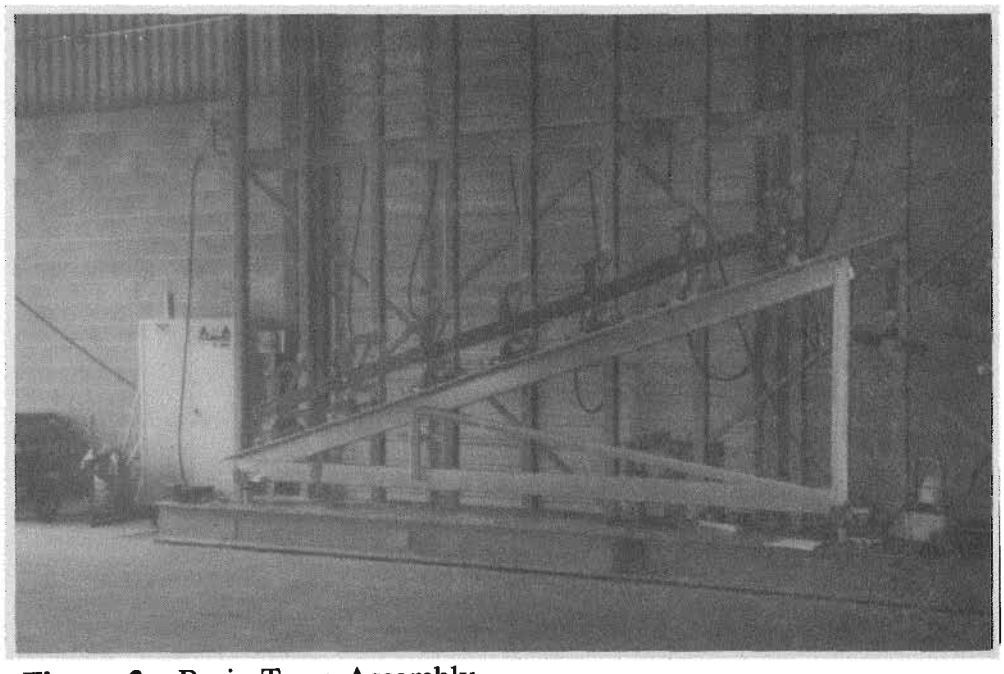

Figure 2. Basic Truss Assembly

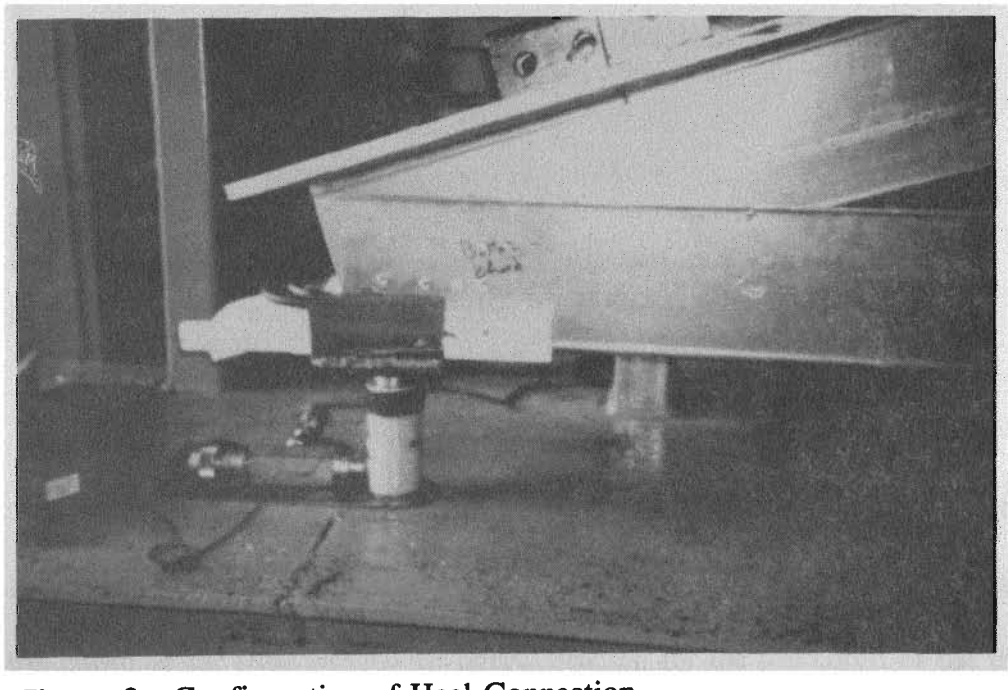

Figure 3. Configuration of Heel Connection

The web members, which spanned between the top and bottom chords, were connected such that the web member C-sections faced the opposite direction as the chord member C-section to which it was connected. The web member was connected to the truss assembly with either four or six self-drilling screws. The number of screws that were used in each individual test is summarized in Table II. Figure 4 illustrates the web to chord connection configuration.

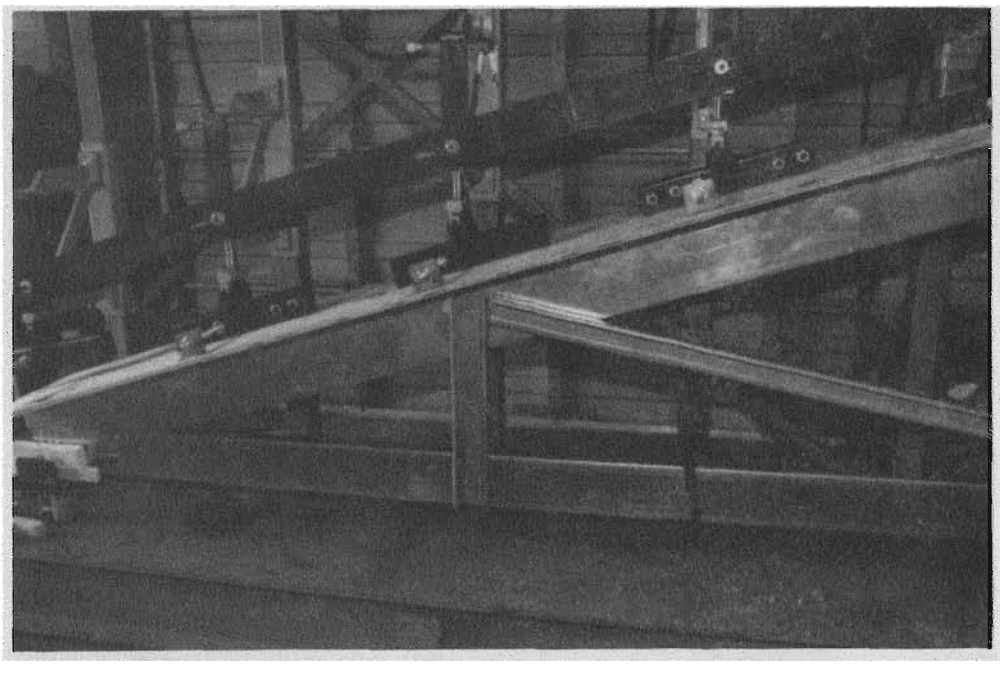

Figure 4. Web to Chord Connection Configuration

Figure 5 shows the truss assembly as it was mounted in the testing frame. Plywood sheathing, measuring 18 inches wide by 3/4 inches thick, was attached to the top chord of the truss to provide lateral bracing for the top chord of the truss assembly. The sheathing was centered on the top chord and connected to the top flange by screws

placed at approximately 12 inch intervals. A series of hydraulic jacks were used to apply a simulated uniform gravity load to the top chord of the truss assembly. The truss assembly was placed in the testing frame so that the line of action of the hydraulic jacks coincided with the centerline of the sheathing; therefore, the line of action of the jacks was centered on the top chord. The hydraulic jacks were then screwed to the sheathing through stabilizer brackets that extended 6 inches to either side of the line of action of the jacks. Figure 6 shows the connection of the hydraulic jacks to the truss assembly. The truss assembly was supported at each end by a load cell. As shown in Figure 7, the truss was braced in the load cell bracket to restrain against out of plane rotation and web crippling.

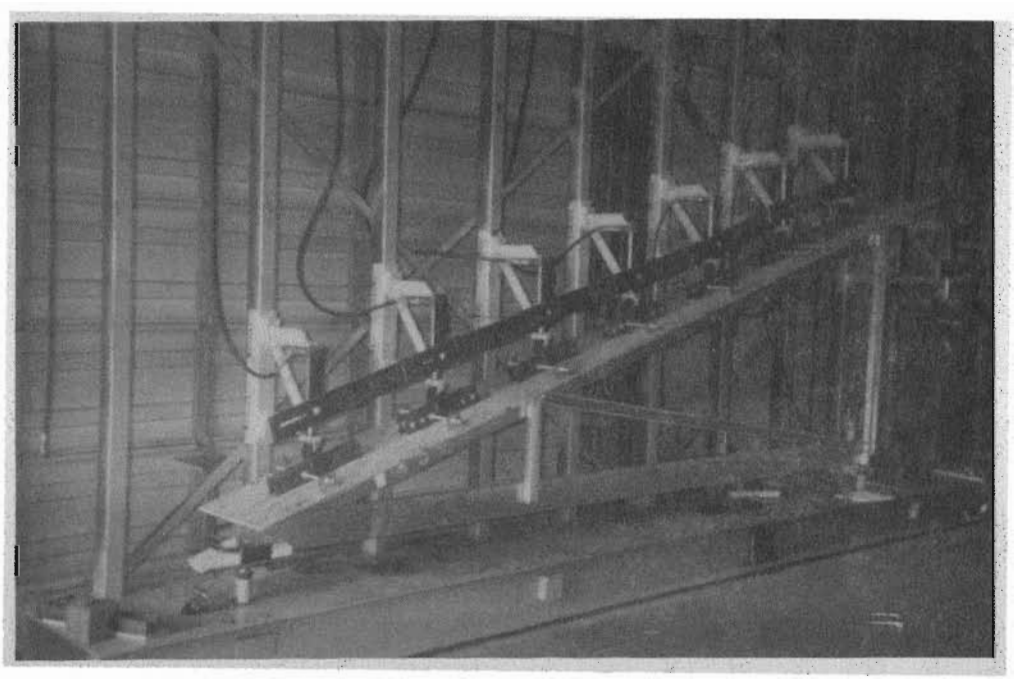

Figure 5. Truss Assemby Mounted in Mitek Test Frame

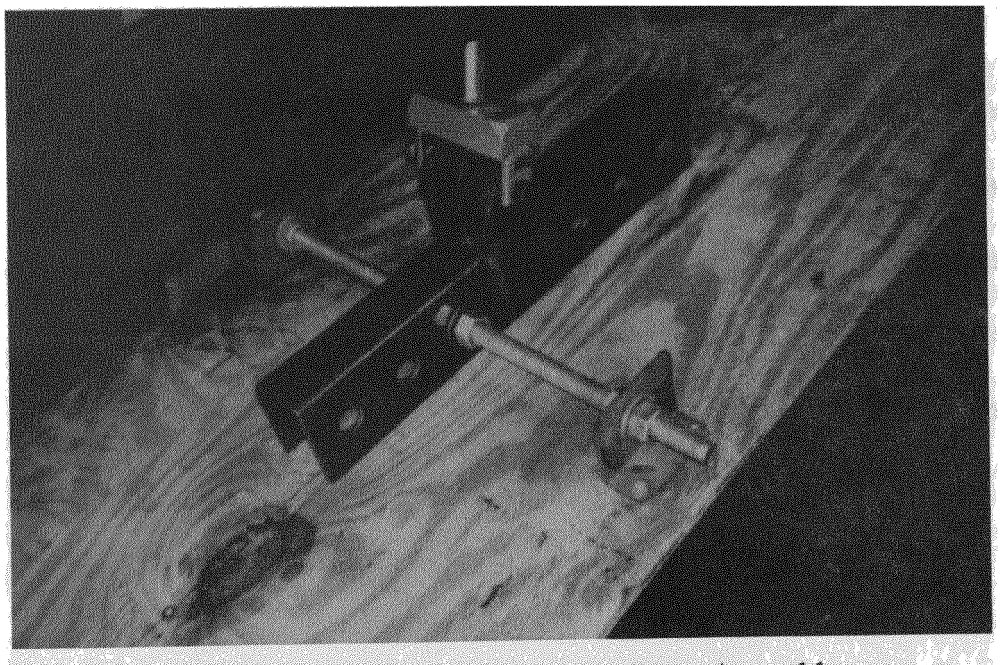

Figure 6. Connection of Hydraulic Jacks to Truss Assembly

Figure 7. End of Truss Assembly Resting on Load Cell

2. Second Series of Tests. The truss assemblies tested at the University of Missouri-Rolla Engineering Research Laboratory were fabricated in the same manner as those used during the first series of tests. However, six self-drilling screws were placed at each end of the compression web member for all tests in this series. The main difference between the truss assemblies used in the first and second series of tests lies in the testing machine used and therefore the method of mounting the truss assemblies in the machine. Figure 8 shows the truss assembly mounted in the University of Missouri-Rolla testing frame.

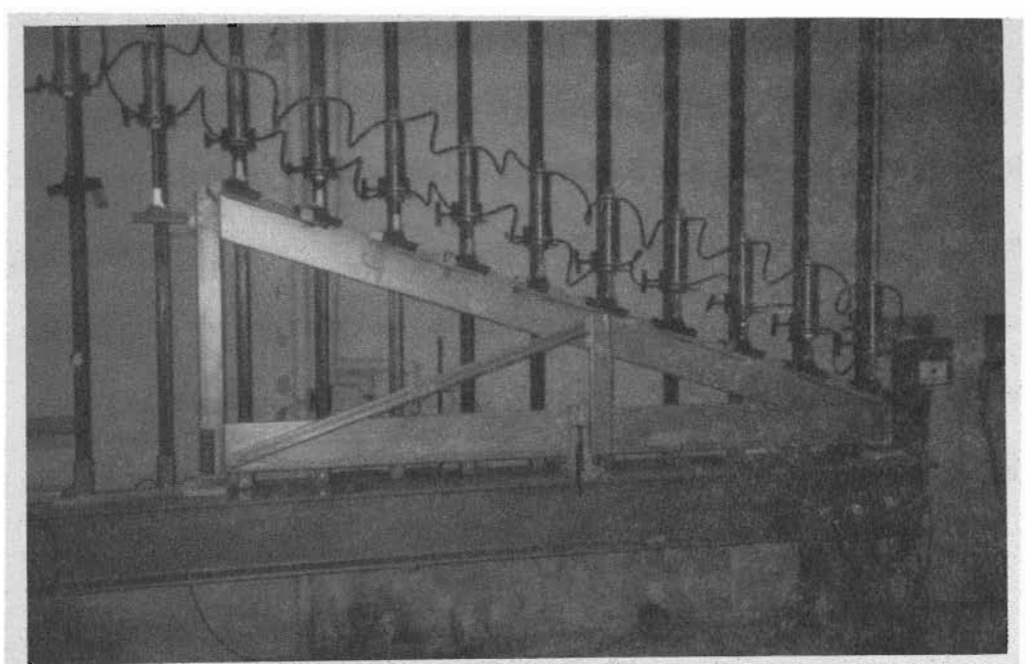

Figure 8. Truss Assembly Mounted in University of Missouri-Rolla Test Frame

In the second series of tests, the truss assembly was supported at both ends by a load cell. As shown in Figure 9, bearing stiffeners and wooden spacers were used to preclude any out-of-plane rotation and web crippling that might occur at the load cells.

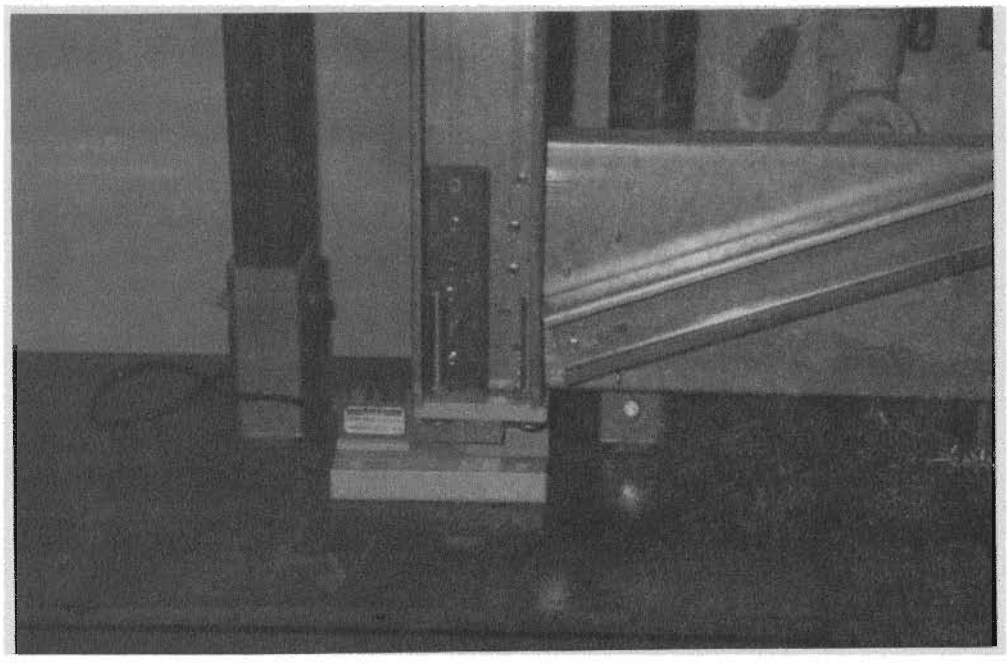

Figure 9. End of Truss Assembly Resting on Load Cell

Pneumatic cylinders spaced at one foot on center were used to apply a simulated uniform gravity load to the top chord of the truss assembly. The connection of the load cylinders to the top chord of the truss was made by the channel sections connected to the bottom of the cylinders. The vertical placement of the cylinders was adjusted so that the channels rested on the top chord of the truss. Wooden surveying stakes were used to prohibit lateral movement of the top chord in the channels. Figure 10 shows the connection of the load cylinder to the truss.

Lateral bracing was employed to prohibit out-of-plane movement of the top and bottom chords. Care was taken to not restrain vertical deflection while laterally restraining the truss assembly. The bottom chord was laterally braced at approximately its mid-span by a wooden brace shown in Figure 11. Bracing of the top flange of the top chord was provided by the connection of the cylinders to the truss as discussed

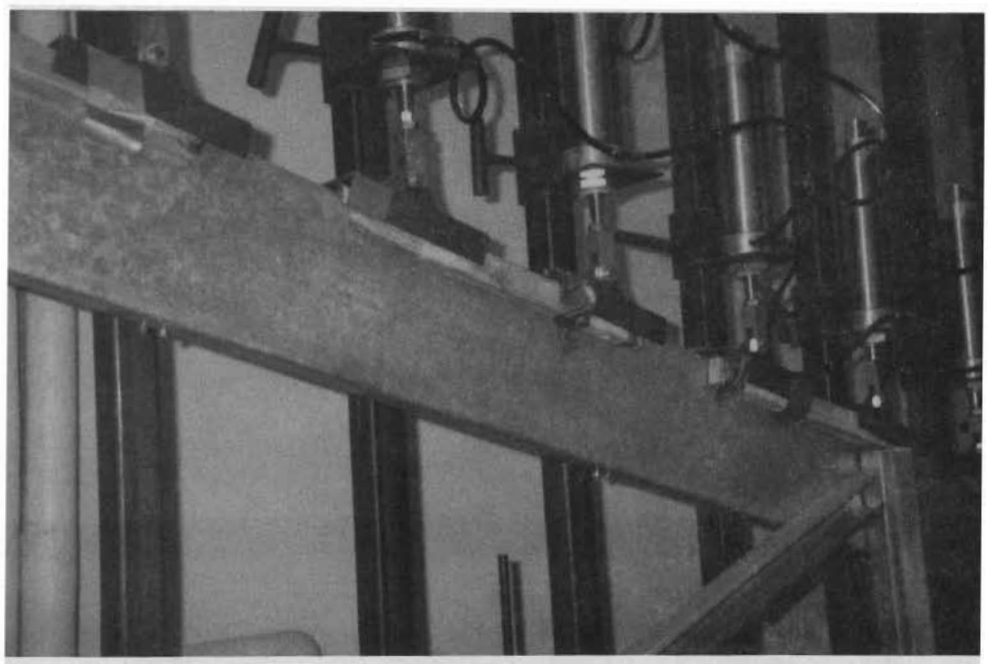

Figure 10. Connection of Load Cylinder to the Truss Assembly

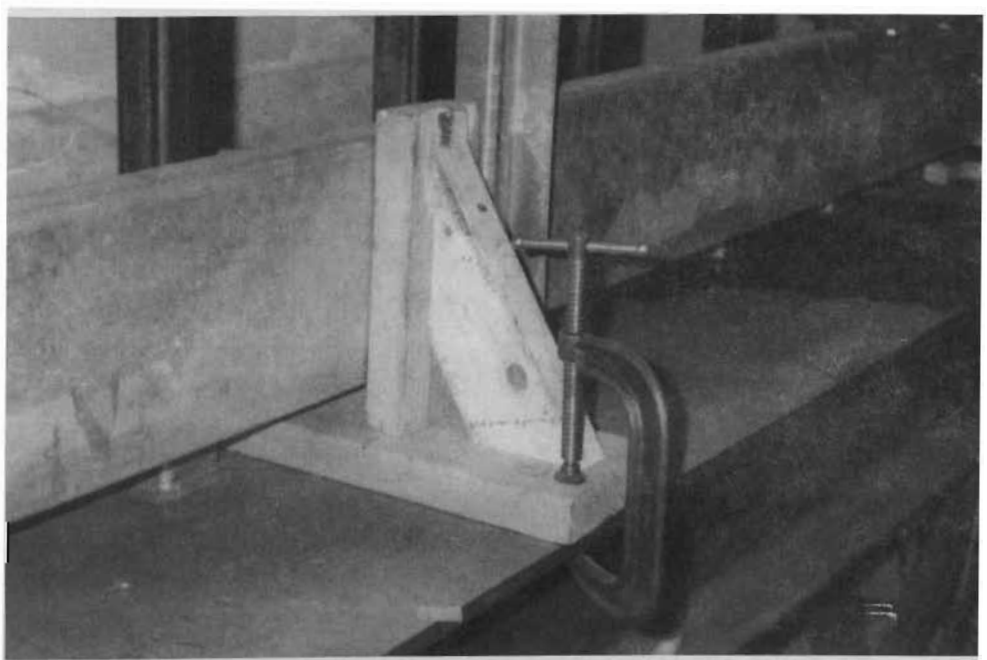

Figure 11. Bottom Chord Lateral Brace

above. The bottom flange of the top chord was restrained against out-of-plane movement by wire ties. At the tie locations, a #10 self-drilling screw was drilled through the bottom flange of the top chord. Sixteen gage steel wire was then used to tie this screw to the vertical posts of the testing machine. This connection, which is shown in Figure 12, allowed vertical deflections of the top chord while holding the bottom flange at a constant distance from the vertical support posts of the testing frame.

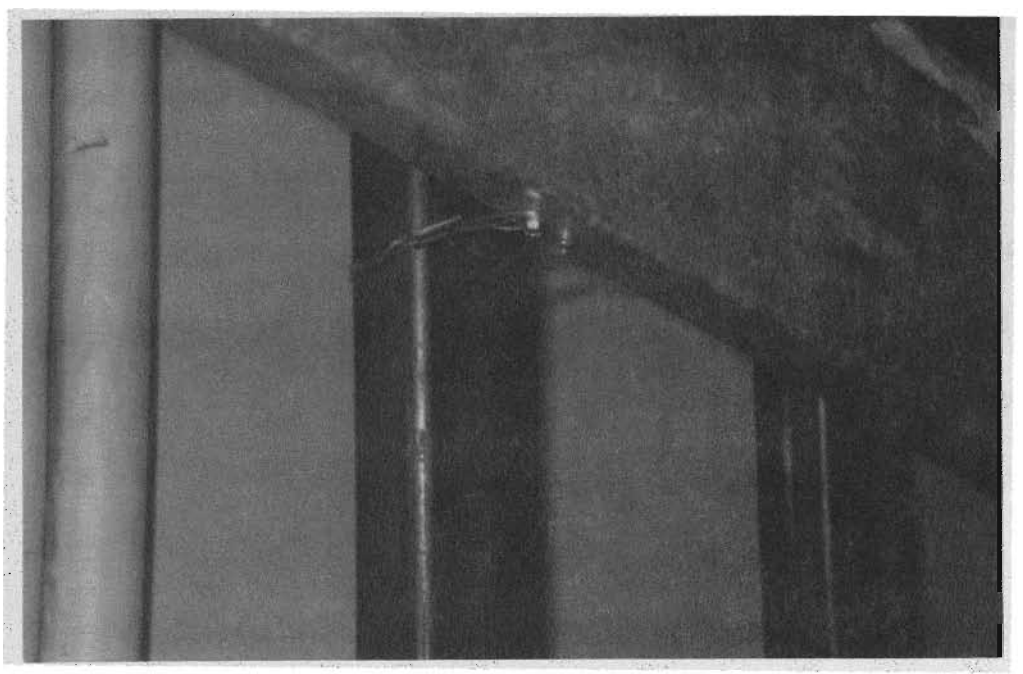

Figure 12. Lateral Brace of the Bottom Flange on the Top Chord

D. DATA COLLECTION

1. First Series of Tests. At each load interval, measurements were taken of the vertical end reactions of the truss assembly and the transverse deflection at the center of the compression web member. The behavior of the entire truss system was visually

inspected during all tests to observe the performance of all individual members and connections.

The vertical end reactions were measured using the load cells that supported the ends of the truss. The load cells digitally displayed the pressure measured in pounds per square inch. These pressure measurements were multiplied by the cross-sectional area of the cell to obtain the reaction forces. Figure 3 in Section III-C shows the load cells used in the first series of tests.

The transverse deflection at the midspan of the compression web member was measured with a dial gauge as shown in Figure 13. Test 14 was the first of the tests performed on members with slenderness ratios of approximately 100. During these tests, excessive rotation of the top chord was observed to cause transverse deflection of the end of the compression web member that was connected to the top chord. Due to this observation, a dial gauge was placed at the connection of the web member with the top chord and these deflections also were recorded. The out of plane slenderness ratio was computed assuming a pin-ended condition such that $K=1.0$.

2. Second Series of Tests. During the series of tests performed at the University of Missouri-Rolla, measurements were recorded for the truss assembly end reactions, and for the compression web member mid-span deflections and strains. Visual inspection of the truss assembly was also performed at each load increment to observe the performance of all individual members and connections.

The truss assembly end reactions were measured to the nearest ten pounds by the load cells that supported the ends of the truss. The mid-span transverse deflection of the compression web member was measured using a dial gage that was placed at that location

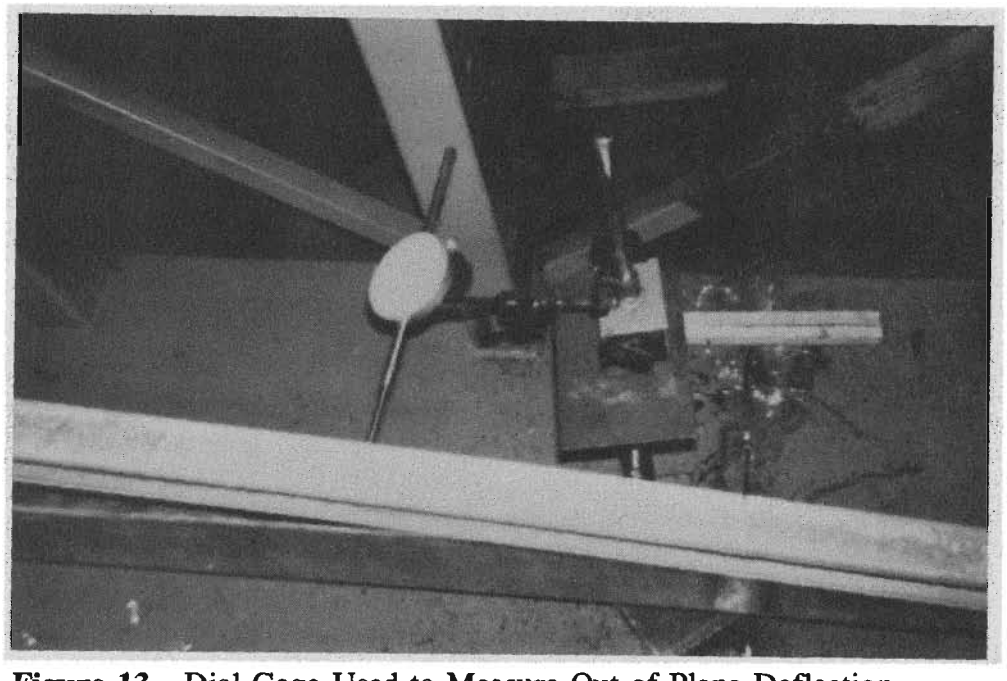

Figure 13. Dial Gage Used to Measure Out-of-Plane Deflection

of the member. The dial gage was placed at mid-depth of the web member to avoid inaccurate measurements if twisting of the section occurred. Figure 14 shows a typical location of the dial gage and strain gages on the compression web member. Measurements of strain at the mid-span of the compression web member were taken at four locations in the cross-section. The locations of the strain gages are shown in Figure 15. Gages 1 and 3 were used to measure the compression strain at the outside and inside faces of the web, respectively. These gages were placed on both sides of the web to determine if local buckling was occurring. Gage 2 was located on the outside face of the flange stiffener to measure the extreme tension fiber strain. Gage 4 was located on the flange at the theoretical centroid of the compression web member in the x-direction. For elastic bending, the centroid and neutral axis coincide; therefore, the intent for Gage 4 was an attempt to measure the axial strain of the member without any contribution

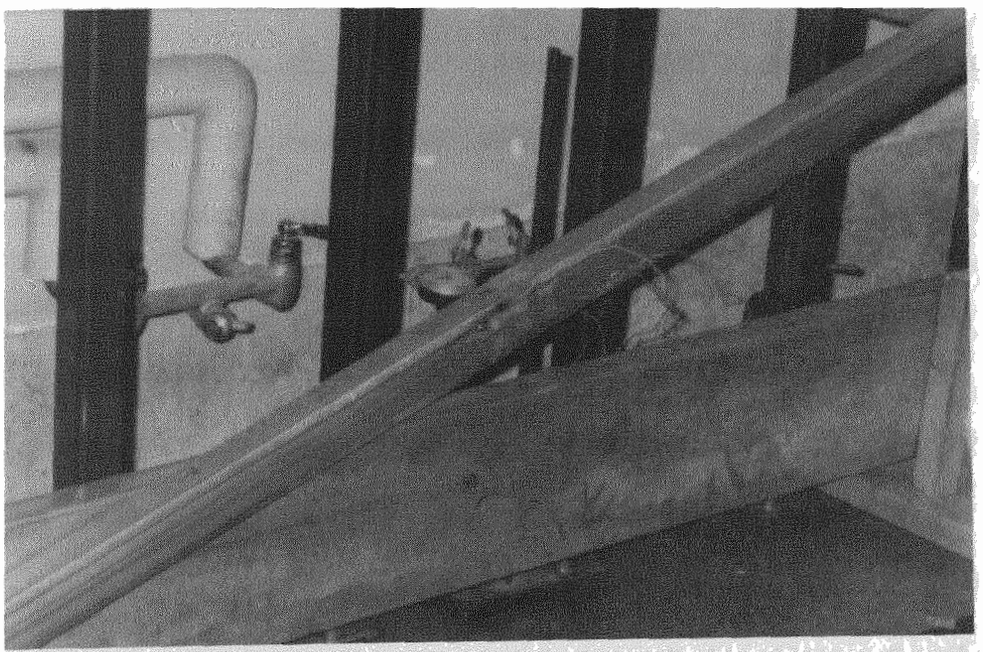

Figure 14. Typical Location of Dial Gage and Strain Gages

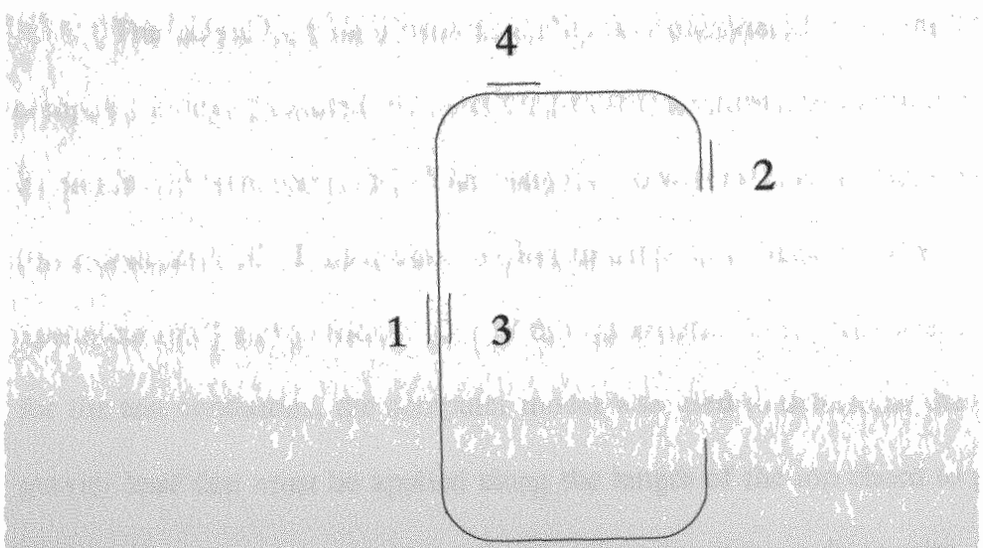

Figure 15. Locations of Strain Gages on Web Member

from bending. Gage 5 was placed at the same location in cross-section as Gage 3; however, it was located 3 ½ inches from the end of the web member that connected to the bottom chord. As with Gage 4, the original intent of Gage 5 was to measure the axial strain without any contribution from bending.

E. EXPERIMENTAL PROCEDURE

1. First Series of Tests. After the truss had been mounted in the testing frame, the initial readings on the dial gauge and load cells were recorded. The loading was applied using a hydraulic system that applied a load every 2 feet along the length of the truss. As can be seen in Figures 4 and 5, the applied load is transferred to the sheathing through a 16 inch long bracket. The sheathing then transfers the load to the top chord of the truss assembly; therefore, the load is assumed to be uniformly applied. The load was incrementally increased with measurements of load and deflection being recorded at each increment. The test was discontinued when a target level of loading on the truss assembly was reached.

The target load on a truss assembly was considered to be the load at which the computer model predicted the axial load in the compression web member was equal to its nominal axial capacity, P_n. The compression web member nominal axial capacity, P_n, for a concentrically loaded compression member is defined in Section C4 of the AISI Specification[3] and Section II-D.1 of this document. Using the axial load P_n calculated for the test conditions, the computer model was used to determine the level of uniform gravity load that must be applied along the length of the top chord to produce an axial load in the compression web member equal to the computed capacity, P_n. The sum of

the vertical reactions at the ends of the truss assembly at this level of uniform gravity load was defined to be the target load for the truss assembly.

This test procedure was performed for three different compression web member lengths. These lengths were chosen corresponding to out-of-plane slenderness ratios of 100, 150, and 180. The slenderness ratio was computed assuming a pin-ended condition such that $K=1.0$. For each of these slenderness ratios, tests were performed for three different thicknesses: 0.0360, 0.0469, and 0.0593 inches. Duplicate tests were performed for each truss geometry. The exception being that no tests were performed for 0.0360 inch thick members with slenderness ratio of 180. These tests were not performed due to the unavailability of the 0.0360 inch thick members at the time that the truss assemblies with slenderness ratio of 180 were being tested in the first series of tests.

Several tests were also conducted to assess the end-restraint provided by the screw connections. For similar member geometries, web members having either four or six screws were load tested. However, after the initial testing showed no difference in the mid-span transverse deflection, this study was discontinued.

2. Second Series of Tests. After the truss assembly was mounted in the testing frame and the compression web member was attached, the resistance of the strain gages was checked using a multimeter. The strain gage wires were then connected to the data acquisition circuitry and the gages were zeroed. Before applying any load, initial readings were taken of the load cell display, dial gage, and strain gages. The load was incrementally increased until failure was achieved in the compression web member. At each load increment, the load cell, dial gage, and strain gage readings were all recorded.

Failure was defined as either a bending failure or when the transverse deflections of the compression web member became unstable. Unstable deflections were considered to occur when the dial gage reading had not stabilized after a period of approximately two to three minutes. Figure 16 shows a bending failure that occurred during Test 20.

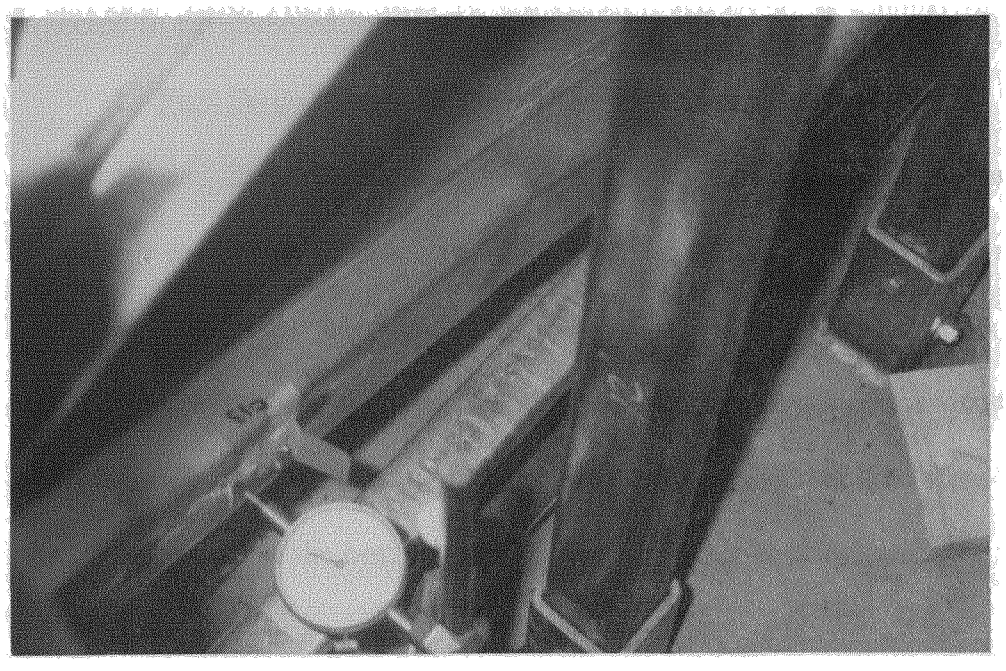

Figure 16. Bending Failure Observed in Test 20

As in the first series of tests, tests were performed for truss assemblies with three different compression web member lengths. These lengths were chosen corresponding to out-of-plane slenderness ratios of 100, 150, and 180. The slenderness ratio was computed assuming a pin-ended condition such that $K=1.0$. For each slenderness ratio, tests were performed for three different thickness: 0.036, 0.0457, and 0.0551 inches.

F. EVOLUTION OF TEST ASSEMBLY

As a result of using hydraulic and pneumatic loading for the first time in this phase of the testing program, it was necessary to make modifications to the test assembly when difficulties were encountered. Care was taken to make all modifications such that the behavior caused in the test assembly would be similar to the behavior that could be expected to be observed in actual truss construction.

1. First Series of Tests. Table II gives the characteristics of each test in the first series of tests. During the performance of the first three tests, it was observed that the entire truss assembly deflected out of plane. To correct this problem, a lateral brace was placed on the bottom chord at a distance of 81 inches from the left support. Figure 17 shows the top and bottom chord lateral braces. It was reasoned that including a lateral brace on the bottom chord would model the lateral restraint offered from the connection of a ceiling board to the bottom chord of a truss. This is also consistent with detail D.5

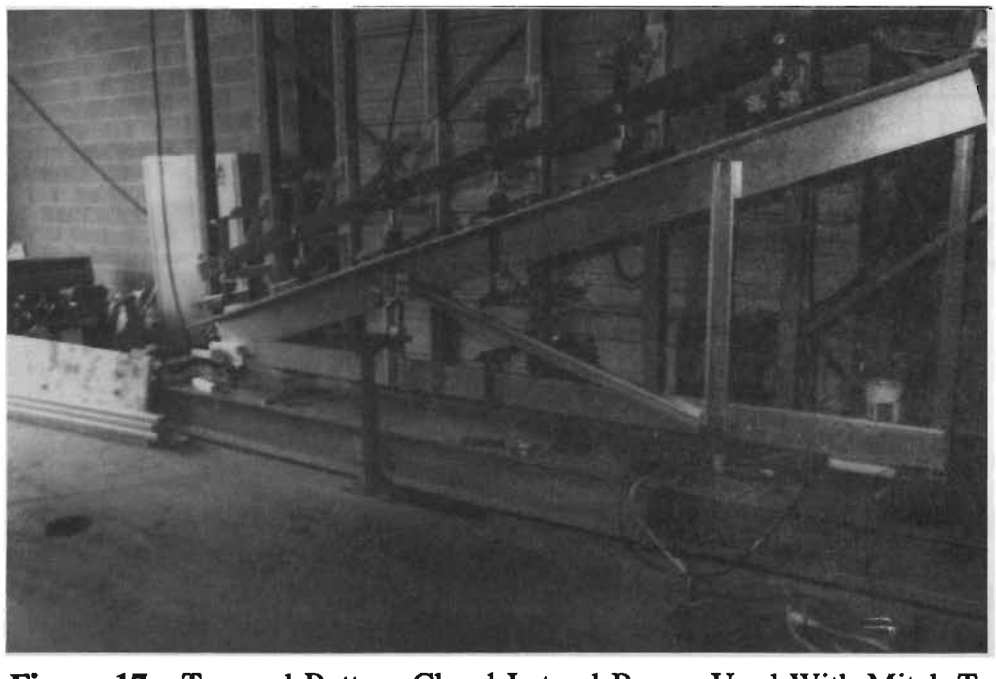

Figure 17. Top and Bottom Chord Lateral Braces Used With Mitek Test Frame

Table II. CHARACTERISTICS OF FIRST SERIES OF TESTS

TEST	LENGTH OF WEB (IN)	SECTION TYPE	NO. OF SCREWS	BOTTOM CHORD BRACE	TOP CHORD BRACE	MID-SPAN DIAL GAGE	PANEL POINT DIAL GAGE
1	109	TYPE I	4			●	
2	109	TYPE I	4			●	
3	109	TYPE I	6			●	
4	109	TYPE I	6	●		●	
5	109	TYPE II	4	●		●	
6	109	TYPE II	4	●		●	
7	109	TYPE II	6	●		●	
8	90	TYPE III	4	●		●	
9	90	TYPE III	4	●		●	
10	90	TYPE I	4	●		●	
11	90	TYPE I	4	●		●	
12	90	TYPE II	4	●		●	
13	90	TYPE II	4	●		●	
14	58	TYPE III	6	●	●	●	●
15	58.5	TYPE III	6	●	●	●	●
16	58.5	TYPE II	6	●	●	●	●
17	58.5	TYPE II	6	●	●	●	●
18	58.5	TYPE I	6	●	●	●	●
19	58.5	TYPE I	6	●	●	●	●

of the AISI "Low Rise Residential[14] Construction Details." Detail D.5 shows "Continuous channel bridging as required" to provide lateral stability. During tests 14 through 19, a lateral brace was connected to the top chord to further restrain out of plane

deflection of the top chord. This is consistent with detail D.6 of the AISI "Low Rise Residential Construction Details." Detail D.6 shows "Continuous channel bridging as required" to provide lateral stability of the top chord.

2. Second Series of Tests. As a result of the lessons learned during the first series of tests, fewer modifications were necessary during this series of tests. Table III shows the characteristics of each test in the second series of tests. During initial testing, a failure occurred in the top chord at the ridge connection. To preclude any future web crippling failures, bearing stiffeners were included at the ridge connection and at both supports. In another initial test, failure occurred in the bottom flange lateral brace placed

Table III. CHARACTERISTICS OF SECOND SERIES OF TESTS

TEST	LENGTH OF WEB (IN)	SECTION TYPE	NO. OF TOP CHORD BRACING POINTS ON BOTTOM FLANGE	STRAIN GAGE LOCATIONS				
				1	2	3	4	5
20	59	TYPE III	2	●	●	●	●	●
21	59	TYPE IV	3	●	●	●	●	
22	59	TYPE V	3	●	●	●	●	
23	90	TYPE III	3	●	●	●	●	
24	90	TYPE IV	3	●	●	●	●	
25	90	TYPE V	3	●	●	●	●	
26	107	TYPE III	3	●	●	●	●	
27	107	TYPE IV	3	●	●	●	●	
28	107	TYPE V	3	●	●	●	●	

at the mid-span of the top chord. Therefore, in Test 20 bottom flange lateral braces were placed at two locations along the length of the top chord. In Test 21 and subsequent tests, bottom flange lateral braces were placed at three locations along the length of the top chord. The lateral bracing of the top chord is described in Section III-C.2.

As described in Section III-D.2, Strain Gage 5 was located 3 ½ inches from the end of the compression web member that connected to the bottom chord. Test 20 showed that a stress concentration existed near the connection; therefore, Gage 5 would not be able to serve its intended purpose of predicting the uniform axial stress throughout the cross-section. In Test 21 and subsequent tests Gage 5 was removed from the study.

IV. COMPUTER MODEL

A. GENERAL

A computer model for each truss assembly was generated using M-STRUDL, a linear elastic, structural analysis program. M-STRUDL is a personal computer version of the mainframe program, STRUDL.

B. ASSUMPTIONS

The truss assembly was modeled in M-STRUDL as a plane frame subjected to a uniform gravity load acting along the length of the top chord. It was necessary to model the truss assembly as a frame instead of a truss so that the chords could be modeled as continuous members. In the development of the model, the top chord was assumed to be continuous from heel-to-ridge. Likewise, the bottom chord was assumed to be continuous from heel-to-heel. This is consistent with the method of fabrication for the truss assemblies in that a single, continuous, C-section was used for each chord. It was assumed in the computer model that all connections between individual members would act as pin connections that are not capable of carrying moments. To model a uniform gravity load along the length of the top chord, the loading was modeled as a uniform vertical load acting downward. M-STRUDL assumes that the uniform load is applied along the center of gravity of the top chord member and that all connections are concentric. Therefore, care must be taken when interpreting M-STRUDL results to properly consider the eccentricities that result in the connections of C-sections.

C. USE OF MODEL

The computer model was used to predict the level of axial load that would be produced in the compression web member when a specified uniform load was applied along the length of the top chord. Since the truss assembly was designed such that the compression web member would be the weakest structural element in the assembly, the capacity of the compression web member should control the capacity of the truss assembly as a whole. Therefore, the failure load of the truss assembly was determined by using M-STUDL to determine the uniform load necessary to produce an axial load in the compression web member equal to its capacity.

The computer model was also used to predict the axial load in the compression web member that resulted from the uniform gravity load applied to the top chord at each increment in the testing program.

V. EVALUATION OF TEST RESULTS

A. GENERAL

A total of 28 full-scale tests were completed in this phase of the University of Missouri-Rolla study of cold-formed steel truss assemblies. The first series of tests consisted of 19 tests with measurements being taken of the end reactions of the truss assemblies and the out-of-plane midspan deflections of the compression web member. Measurements were taken of the out-of-plane deflections at the connection of the compression web member to the top chord in Tests 14 through 19. The second series of tests consisted of nine tests with measurements being taken of the end reactions of the truss assemblies and the out-of-plane deflections and strains at the midspan of the compression web member.

Evaluation of the test results consisted of a correlation of the computer model to the experimental results and a comparison of the experimentally determined capacity to the capacity predicted by the AISI Specification[3]. The correlation of the computer model to the experimental results is presented in this document by two different methods. The purpose of these two methods is to explain why the observed extreme fiber stresses and the observed out-of-plane deflections are consistently less than the predicted values. Since these stresses and deflections are functions of the moment about the weak axis of the compression web member, it was reasoned that a mechanism must exist that reduces the moment diagram along the length of the member.

1. End Moment Mechanism. The first of the two methods is referred to as the End Moment Mechanism. It was assumed in the calculation of the stresses and

deflections that the ends of the compression web member were connected to the chords of the truss assembly by perfect pin connections. A perfect pin connection implies that the connection cannot carry a moment; however, in reality the connection to the chords will offer some end restraint to the compression web member depending upon the relative stiffness' of the members and the geometry of the connections. In this testing program the truss assembly was designed so that the compression web member would be the critical member. This required that the chord members be over-designed relative to an optimally designed truss assembly. Because of this relatively high stiffness of the chord members it is reasonable to believe that there could be significant end restraint provided to the compression web member. The end restraint provided to the compression web member causes a negative moment to occur at the support. As shown in Figure 18, the negative moment caused at the support acts to shift the moment diagram downward which causes a lower moment at the mid-span of the compression web member.

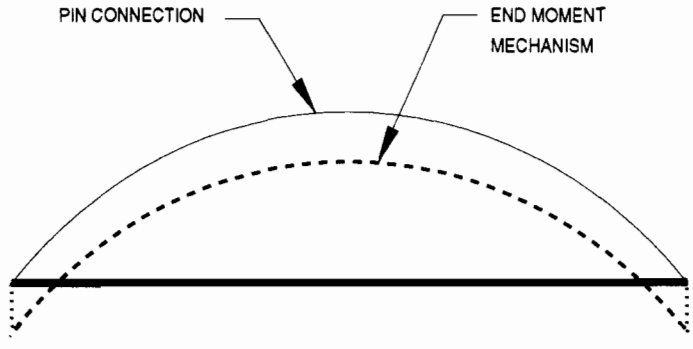

Figure 18. Downward Shift in Moment Diagram Due to End Restraint

2. Tension Force Mechanism. The second of the two methods for the correlation of the computer model to the experimental results is referred to as the Tension Force Mechanism. Because the compression web member deflects out-of-plane without much in-plane deflection, it was proposed that a tension force had been produced in the compression web member. This tension force, in effect, reduces the applied axial compression load in the web member. To study this theory further, the ends of the compression web member were assumed to be perfect pin supports in that they could not translate nor resist moments. Information regarding the translation of the ends of the member was not recorded during the experimentation; however, visual inspection of the truss assembly under load indicated that very little vertical deflection occurred until the ultimate load of the truss was approached. Based upon the assumption that the ends of the member are perfectly pinned, the tension force was computed by calculating the increased length of the compression web member caused by the out-of-plane deflection and comparing it to the original length of the member. The amount of increase in the length was used to calculate the strain and then the stress, T, that caused this elongation. This tension stress, T, was then used to modify the axial compression force, P, predicted by the computer model. Equation 6 defines the modified axial force, P_{mod}.

$$P_{mod} = \left(-\frac{P}{A} + T\right) \cdot A \qquad (6)$$

where P = Axial force in compression web as predicted by computer model

A = Full cross-sectional area of the compression web member

Since the axial compression load, P, predicted by the computer model is negative, the result of adding the tension stress, T, to the axial compressive stress, P/A, is that the modified compression load, P_{mod}, is lower that P.

B. CORRELATION OF EXTREME FIBER STRESSES

Strain gage capability was only available for the second series of tests; therefore, discussion of extreme fiber stresses produced in the compression web members is limited to Tests 20 through 28. The strain data from the gages located at mid-span of the compression web member was used to compute the extreme bending fiber stresses for minor axis bending. These experimentally determined stresses were compared to the predicted stresses calculated using the computer model. The predicted stresses were computed assuming superposition of the axial stress and the bending stress that results from the eccentric connections in the truss assemblies. The eccentricity arises from the load being applied at the web of the C-section as opposed to at the center of gravity. Additionally, this eccentric loading causes a bending moment which results in an out-of-plane deflection, Δ, which further increases the eccentricity. The eccentricities are graphically shown in Figure 19 . The extreme compression fiber stress was computed using Equation 7.

$$\sigma_c = \frac{P}{A} + \frac{P(e+\Delta)}{S_{yc}} \qquad (7)$$

where e = Dimension defined by Figure 19

Δ = Experimentally measured deflection when axial load equals P

S_{yc} = Full section modulus of extreme compression fiber in minor axis bending

Figure 20 shows a typical plot of the experimentally determined stresses and the predicted stresses as a function of the total load that was applied to the truss assembly. The rest of these plots for the second series of tests are shown in Appendix B. It was concluded that this method of computing the stresses consistently over-estimated the level of stress in the extreme compression fiber. The extreme tension fiber stress was computed using the same method and a similar trend was observed in that the computed tension stresses consistently over-estimated the level of stress in the extreme tension fiber. The two methods of interpreting the deviation between the predicted stresses and observed stresses are presented below.

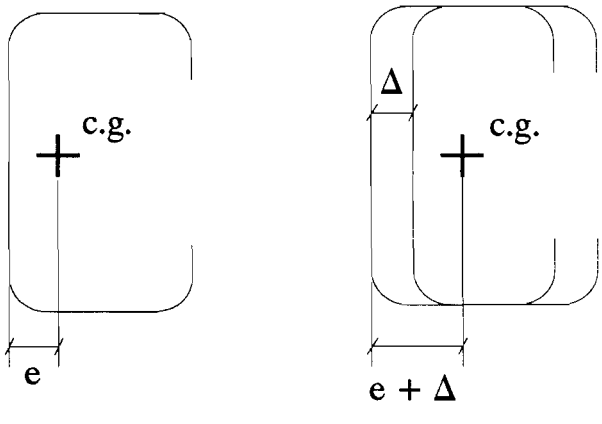

Figure 19. Definition of Eccentricities

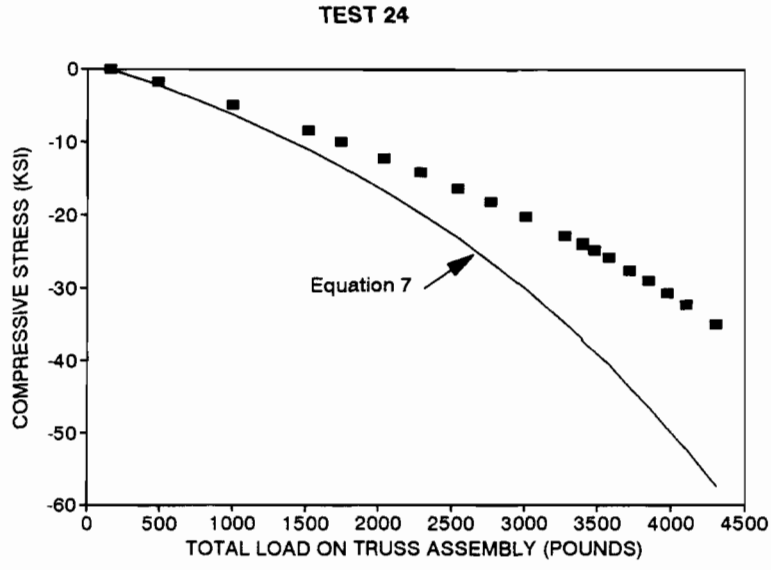

Figure 20. Experimentally Determined Compression Stress Vs. Predicted

1. End Moment Mechanism. Equation 7 shows that the extreme compression fiber stress at any point along the length of the member is equal to the sum of the axial component and the bending component. The axial component of the stress will be constant along the length of the member; however, the bending component at any location along the length of the member is a function of the bending moment at that location. As displayed in Figure 18, the restraint moment at the ends of the compression web member will shift the bending moment diagram downward. This downward shift results in the bending moment at the mid-span of the compression web member being lower than if there was not a restraint moment present. Since, in this testing program the chord members were relatively stiff, it is reasonable to expect that a restraint moment is present that causes the bending moment to be lower at the mid-span of the compression web member than if no restraint moment was present. This would cause the compression

stress at the mid-span to be lower than if the ends were perfectly pinned as was assumed. This is in agreement with the observation in the testing program that the extreme fiber stresses were consistently lower than was predicted by assuming the connection of the compression web member to the chords were perfectly pinned. Figure 21 shows a typical plot of the magnitude of the end restraint moments necessary to make the predicted extreme compression and tension fiber stresses agree with the experimentally determined values. The necessary restraint moment, M_{end}, was calculated by multiplying the difference between the predicted stress, σ_c, and the experimentally determined stress, σ_{obs}, by the section modulus, S, corresponding to the appropriate extreme fiber. Equation 8 was used to calculate the necessary restraint moment to correct the extreme compression fiber stress prediction.

$$M_{end} = (\sigma_c - \sigma_{obs}) \cdot S_{yc} \qquad (8)$$

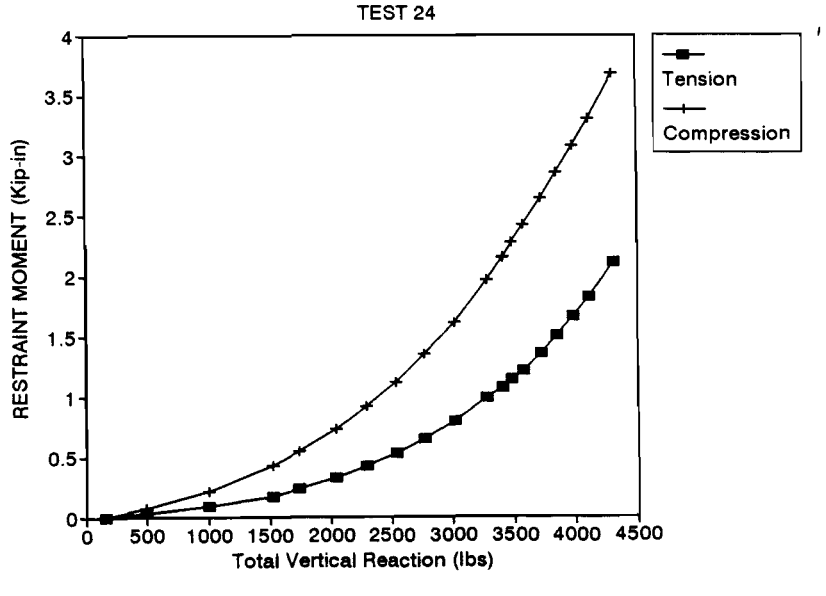

Figure 21. Restraint Moment Necessary to Correct Predicted Stresses

2. Tension Force Mechanism. As discussed in Section V-A.2, the Tension Force Mechanism method of interpreting the results of the experimental study proposes that a tension force reduces the axial load that the compression web member is carrying to a modified axial load, P_{mod}. After substituting the modified force, P_{mod}, for the axial force, P, the extreme fiber stresses were calculated using Equation 7. Figure 22 shows the modified extreme compression fiber stress prediction superimposed upon the graph displayed in Figure 20. This model provides reasonable correlation of the predicted stresses and experimentally determined stresses throughout the early part of the tests. The reasonable correlation is continued past the assumed failure loads that were based upon the compression web members developing axial forces equal to the axial compressive capacities, P_n, for the conditions of each test. For example, the assumed failure load is 2340 pounds for Test 24, which is displayed in Figure 22. The fact that

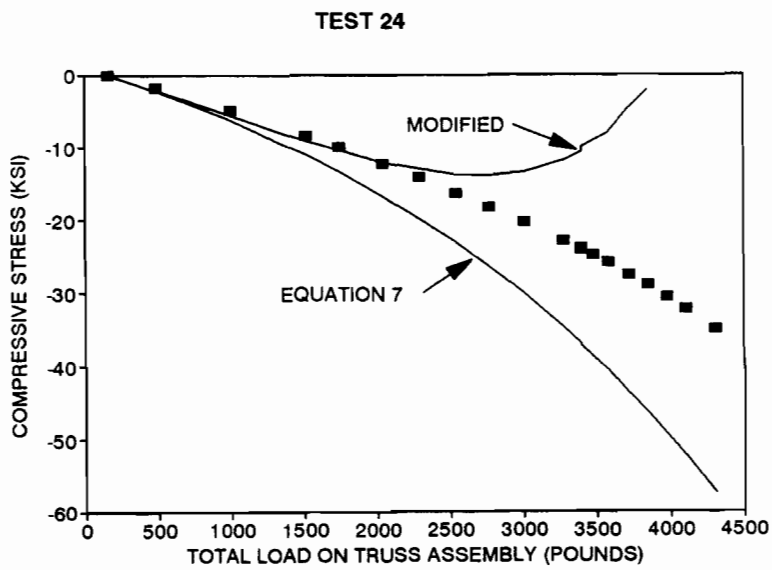

Figure 22. Modified Compression Stress Superimposed on Figure 20

the computed stresses deviate from the experimental stresses at levels of loading near the ultimate load is reasonable, considering that the truss assembly underwent deflections both in-plane and out-of-plane as the ultimate load was approached. These deflections near ultimate load, significantly differ from the assumption that the ends of the compression web member were pin supported.

C. CORRELATION OF OUT-OF-PLANE DEFLECTIONS

Out-of-plane deflections at the mid-span of the compression web member were measured at each load increment for the tests. The experimentally measured deflections were compared to the predicted deflections calculated using the computer model. The mid-span deflection, Δ, of the compression web member was predicted by superimposing an initial deflection, δ_o, and a second order deflection, $\delta_{p\Delta}$. The initial deflection is caused by the end moments created by the eccentric loading. Since the eccentricity is the same at both ends, the moment, $M_o=Pe$, will be constant along the length of the member. Equation 9 was used to calculate the initial deflection at the mid-span.

$$\delta_o = \frac{PeL^2}{8EI_y} \tag{9}$$

where P = Axial force in compression web as predicted by computer model

e = Dimension defined by Figure 19

L = Length of compression web between centers of screw patterns

E = 29500 ksi, Modulus of elasticity for cold-formed steel

I_y = Full moment of inertia for compression web about weak axis

The calculation of the second order deflection was based upon the assumption that the deflected shape of the compression web member would be parabolic. The moment produced by the P-Delta effect, $M_{p\Delta}=P\delta_o$, will vary along the length of the member because the initial deflection will vary along the length of the member. Since the deflected shape of the web member was assumed to be parabolic, the second order deflection at mid-span is given by Equation 10.

$$\delta_{P\Delta}=\frac{5}{48}\frac{(P\delta_o)L^2}{EI_y} \qquad (10)$$

The calculation of the second order deflections was carried out through several increments until convergence was reached. Figure 23 compares the observed deflections to those predicted by this method. As with the prediction of the extreme tension and compression fiber stresses, the prediction of the deflections over-estimated the observed

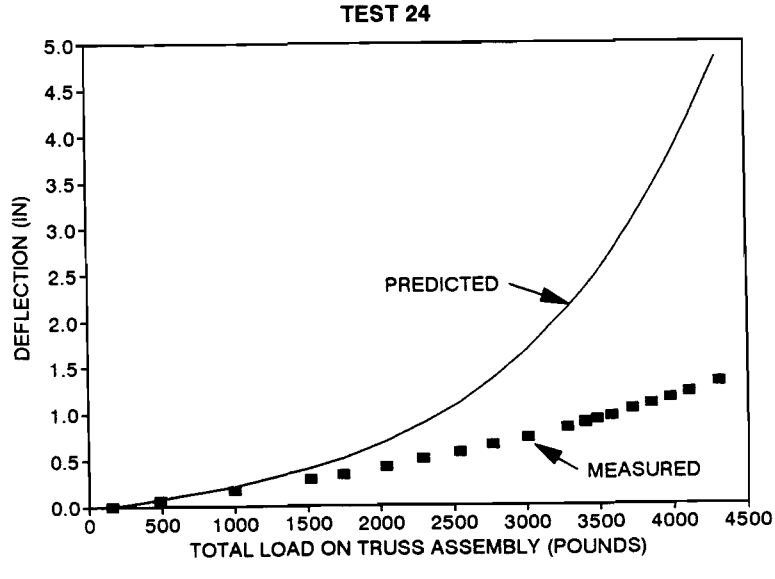

Figure 23. Observed Deflections Vs. Predicted Deflections

deflections. The two methods of interpreting the deviation between the predicted deflections and observed deflections are presented below.

1. End Moment Mechanism. As previously discussed, the mid-span deflection of the compression web member is caused by the bending moment along the length of the member. As can be seen in Figure 18, the presence of an end restraint moment acts to reduce the bending moment along the length of the compression web member. Therefore, this will reduce the amount of deflection that is caused at the mid-span of the member. Also, it intuitively makes sense that if there is an end moment resisting rotation of the ends of the compression web member, the deflection along the length of the member will not be as great as if there was not a restraint moment present. This is in agreement with the fact that throughout the testing program the observed mid-span deflections were less than those predicted assuming that the ends of the compression web member were perfectly pinned. Figure 24 shows a typical plot of the magnitude of the end restraint moment necessary to make the predicted deflections agree with the observed deflections. Equation 11 was used to calculate the necessary restraint moment to correct the deflection prediction.

$$M = \frac{8EI_y}{L^2} \cdot (\Delta - \Delta_{obs}) \qquad (11)$$

2. Tension Force Mechanism. Equations 8 and 9 show that the mid-span deflection of the compression web member is caused by out-of-plane bending moments that are functions of the axial load in the member. As discussed above, the presence of a tension force would reduce the applied compression load in the member to a modified

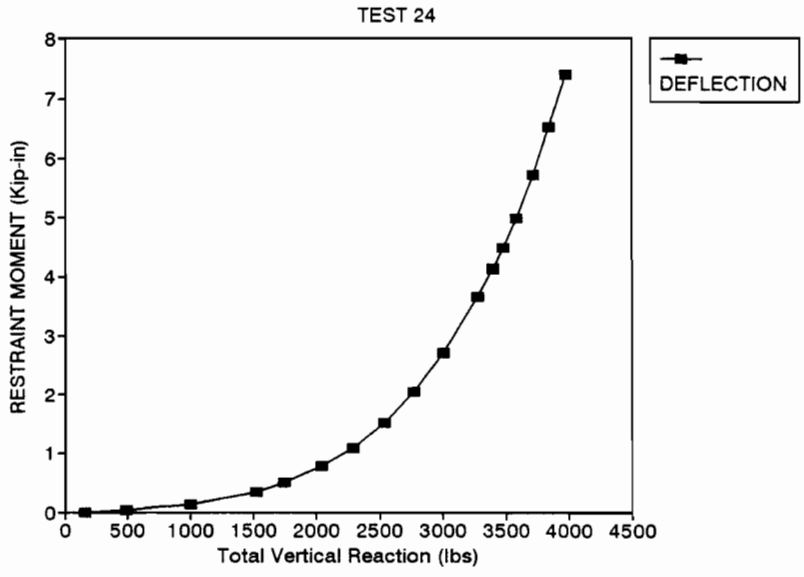

Figure 24. Restraint Moment Necessary to Correct Deflection Prediction

axial compression force, P_{mod}. Therefore, the reduction of the axial load carried by the compression web member would cause the out-of-plane deflection it caused to be reduced. Figure 25 shows a typical example of the modified deflection prediction superimposed upon the graph displayed in Figure 23.

The same trend exists as seen in the calculation of the extreme fiber stresses by the Tension Force Mechanism method. The modified prediction provides reasonable correlation with the measured deflections throughout the early part of the test; however, the predicted deflections deviate from the measured deflections near ultimate loading. This could be attributed to the fact that the truss assembly underwent deflections as the ultimate load was approached that significantly differs from the assumption that the ends of the compression web member were pinned supports.

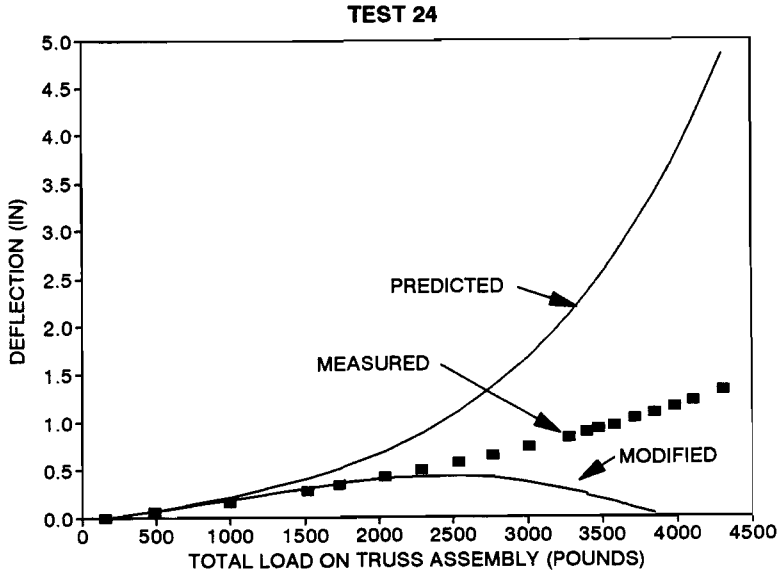

Figure 25. Modified Deflection Prediction Superimposed on Figure 23

D. CORRELATION OF AXIAL FORCES

In an attempt to separate the axial load component of the stress from the minor axis bending stress, a strain gage was placed on the flange of the web member at the theoretical centroid in the x-direction. See Figure 15 for the location of this strain gage in the cross-section. For elastic bending, the centroid and neutral axis coincide; therefore, this gage should be able to measure the axial strain of the member without any contribution from bending. The strain measured by this gage was used to calculate the stress at this point in the cross-section. This stress was assumed to be the contribution from the axial load, P/A; therefore, it was multiplied by the cross-sectional area to calculate an estimate of the axial load based upon the experimental measurements. Figure 26 shows a typical plot of the axial load computed from the experimental

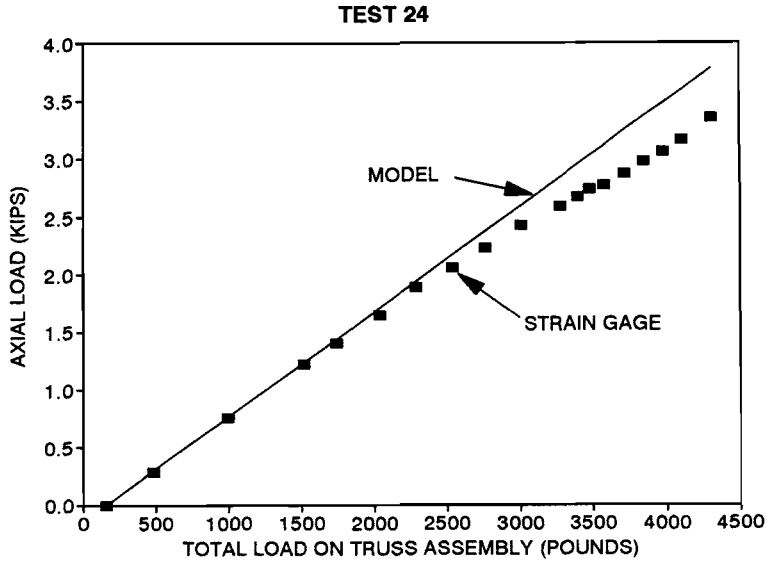

Figure 26. Measured Axial Load Vs. Predicted Axial Load

measurements compared to the axial load predicted by the computer model. As shown in Figure 26, the axial load measured by this procedure shows good correlation with the computer model. To be consistent with the methods of interpreting the exterior fiber stresses and the deflections, the effects of the two methods on the correlation of the axial load are discussed below.

1. End Moment Mechanism. The presence of a restraint moment at the ends of the compression web member would not affect the axial load carried by the member. As was discussed in Section V-A.1, the out-of-plane bending moment would be reduced by the presence of an end restraint moment. This reduction in the out-of-plane moment was responsible for the reduction in the exterior fiber stresses and mid-span deflections compared to the those predicted assuming that the connections of the compression web member to the chords were perfectly pinned. The End Moment Mechanism method does

not propose any change to the axial load the compression web member carries. Therefore, the good correlation of the measured axial load and the axial load predicted by the computer model is in agreement with the End Moment Mechanism method of interpreting the results.

2. Tension Force Mechanism. As discussed in Section V-A.2, the Tension Force Mechanism method of interpreting the results of the experimental results predicts that the axial load carried by the compression web member is reduced to a modified axial load value, P_{mod}. Figure 27 shows a typical plot of the modified axial load predicted by the Tension Force Mechanism method superimposed on the plot in Figure 26. There is poor correlation between the modified axial load, P_{mod}, and the axial force measured using the strain gage located at the theoretical neutral axis for minor axis bending. However, the calculation of the axial load from the stress at Strain Gage 4, is based upon the

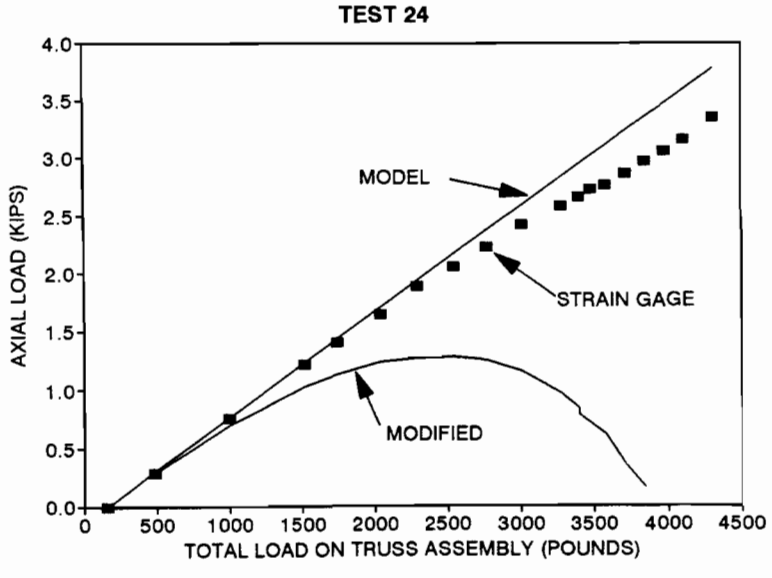

Figure 27. Modified Axial Load Prediction Superimposed on Figure 26

assumption that the neutral axis of the compression web member remains at the location of this strain gage. Due to the relatively large deflections observed in the testing program, it is difficult to know for sure if this assumption is valid.

E. COMPARISON OF OBSERVED CAPACITY TO AISI SPECIFICATION

The second phase of the evaluation of test results was to compare the experimentally observed failure load to the design capacity calculated using the AISI Specification[3]. In the testing program, failure was defined as either a bending failure or when the transverse deflections of the compression web member became unstable. Unstable deflections were considered to occur when the dial gage reading had not stabilized after a period of approximately two to three minutes. Failure was achieved in two of the nineteen tests in the first series of tests and eight of the nine tests in the second series of tests.

In the first series of tests, failure was not achieved in the compression web member in the remaining seventeen tests due to insufficient strength of the top chord. The loading on the truss assembly was increased to the load corresponding to Load Case A, which is described below, and then the top chord was visually inspected. If the top chord was determined to be close to failure, the test was discontinued. If the top chord was secure, the loading was continued until the top chord appeared to be close to failure. In the second series of tests, failure was not achieved in Test 22 due to the lack of available capacity in the University of Missouri-Rolla testing frame. Table IV gives the observed failure loads. If failure was not achieved in a test, the value in the observed

failure load column is marked with an asterisk, *, and will correspond to the highest load applied to the truss assembly during that test.

The compression web member nominal axial capacity, P_n, for a concentrically loaded compression member is defined in Section C4 of the AISI Specification[3] and Section II-D.1 of this document. Using the axial load, P_n, calculated for the test conditions, the computer model was used to determine the level of uniform gravity load that must be applied along the length of the top chord to produce an axial load in the compression web member equal to the computed capacity, P_n. It was observed in the testing program that most of the truss assemblies were capable of supporting the level of loading corresponding to the capacity of the compression web member being determined as a concentrically loaded compression member. This level of loading is represented as Load Case A in Table IV.

The evaluation of the capacities based upon the AISI Specification[3] showed that the capacities of several of the compression web members were controlled by torsional-flexural buckling. However, observations throughout the testing program showed that the controlling behavior for all tests was flexural buckling about the weak axis. The eccentric nature of the load application, which induced minor axis bending, is believed to have forced the minor axis buckling behavior. The minor axis buckling behavior does not produce shear flows that would cause twisting of the section; therefore, torsional-flexural buckling is not a possible failure mode in this situation. To recognize that flexural buckling about the weak axis was the controlling behavior, the capacity of the compression web member for each test was calculated using the AISI Specification but recognizing that the C-section was not subject to torsional-flexural buckling. Again, the

computer model was used to determine the level of uniform gravity load that must be applied to produce an axial load in the compression web member equal to the new computed capacity. This level of loading is represented as Load Case B in Table IV. As discussed previously, failure was defined as either a bending failure or when the transverse deflections of the compression web member became unstable. In Table IV, the observed failure loads for tests that failed due to unstable deflections are marked with a dot, •. In the tests that unstable deflections was the type of failure observed, the truss assembly was subjected to higher levels of loading than recorded as the observed failure load. The observed failure load did not reach the level of loading defined as Load Case B in any of the tests. However, in five of the nine tests completed in the second series of tests, the truss assembly was capable of supporting Load Case B with excessive deflections. Complete load-deflection histories are given in Appendix C.

As discussed in Section V-B, the compression web members in cold-formed steel truss assemblies were observed to behave as beam-columns. The AISI Specification[3] requires beam-columns to meet the conditions of interaction equations C5-1 and C5-2, shown in this document as Equation 4 and 5, respectively. As discussed in Section II-D.2, Equation 4 is used to check stability away from the ends of the member and Equation 5 is used to check yielding at the ends of the member. Since the predominate behavior observed in this testing program was out-of-plane deflections due to the eccentric loading, Equation 4 is the appropriate interaction equation to consider. Therefore, according to the AISI Specification, the maximum load that should be applied to the compression web member would correspond to the loading at which Equation 4 has a value of 1.0. To evaluate the predicted failure load for the compression web

member, the factors of safety were removed from Equation 4 to give Equation 12 shown below.

$$INTERACTION = \frac{P}{P_n} + \frac{C_{mx}M_x}{M_{nx}\alpha_x} + \frac{C_{my}M_y}{M_{ny}\alpha_y} \qquad (12)$$

In Equation 12, P_n is the nominal axial capacity from the AISI Specification[3] for sections not subject to torsional or torsional-flexural buckling. All other variables are defined in Section C5 of the AISI Specification and Section II-D.2 of this document. For this testing program, the predicted failure load based upon the AISI Specification was taken to be the loading at which the Interaction value defined in Equation 12 has a value of 1.0. This level of loading is represented as Load Case C in Table IV.

The results of this experimental study show that the interaction values of Equation 12 are consistently greater than 1.0 at the observed failure load. Table V summarizes the relationship between the observed failure loads, P_{Obs}, and the predicted failure loads, P_{AISI}. The predicted failure loads were based upon Equation 12 equaling 1.0. Columns 1 and 2 of Table V give the values of deflection and axial force, respectively, at the predicted failure load. The values of deflection, axial load and Equation 12 at the observed failures are given in columns 3, 4, and 5 of Table V, respectively. To give a sense of the relative magnitudes of deflections at predicted failure and observed failure, the ratio of these two deflections is given in column 6. Column 7 gives the same ratio for the axial loads. Column 8 gives the ratio of the axial load in the compression web member at the observed failure to the axial load at the predicted failure. This column shows that in every test in which failure was achieved in the compression web member,

Table IV. LEVELS OF TOTAL LOADING ON TRUSS ASSEMBLY

Test	Observed Failure Load (lbs)	Predicted Failure Loads (lbs)		
		Case A	Case B	Case C
1	*1700	1450	2140	1210
2	*1790	1450	2140	1200
3	*1700	1450	2140	1200
4	*1720	1450	2140	1200
5	*1570	2200	2700	1480
6	*2010	2200	2700	1480
7	*2010	2200	2700	1480
8	*1810	1740	3240	1450
9	*2010	1740	3240	1450
10	*2370	2070	3420	1730
11	*2190	2070	3420	1740
12	*3040	3060	4340	1920
13	*3060	3060	4340	1920
14	4320	4500	6700	2600
15	4410	4500	6700	2580
16	*6350	6780	11330	4210
17	*6330	6780	11330	4200
18	*4790	4880	9160	3780
19	*5480	4880	9160	3780
20	5410	4550	7000	2850
21	•7750	5400	10890	4520
22	* 8460	6600	13120	5600
23	•2440	1880	3500	1650
24	•3280	2340	4100	1920
25	•4040	2960	4700	2640
26	•2210	1280	2270	1340
27	•2030	1630	2560	1660
28	•2520	2160	3040	2010

Table V. COMPARISON OF PREDICTED MEMBER FAILURE LOADS TO OBSERVED MEMBER FAILURE LOADS

Column	1	2	3	4	5	6	7	8	9
	Values at Predicted Failure		Values at Observed Failure			Ratios of Predicted Values to Observed Values			Equiv. Defl. Limit
Test	Δ_{AISI} (in)	P_{AISI} (Kips)	Δ_{Obs} (in)	P_{Obs} (Kips)	Equation 12	$\frac{\Delta_{AISI}}{\Delta_{Obs}}$	$\frac{P_{AISI}}{P_{Obs}}$	$\frac{P_{Obs}}{P_{AISI}}$	
14	0.37	1.95	0.80	3.09	1.85	0.46	0.63	1.59	157
15	0.40	1.94	0.93	3.21	1.98	0.43	0.60	1.67	147
20	0.21	1.93	0.68	3.85	2.74	0.31	0.50	2.00	281
21	0.34	3.21	0.77	5.60	2.71	0.44	0.57	1.75	174
23	0.34	1.31	0.68	1.82	1.68	0.50	0.72	1.39	265
24	0.48	1.89	0.82	2.59	1.85	0.59	0.73	1.37	188
25	0.50	2.38	0.89	3.27	1.97	0.56	0.73	1.37	180
26	0.34	1.07	0.85	1.76	3.24	0.40	0.61	1.64	315
27	0.36	1.46	0.52	1.84	1.53	0.70	0.79	1.27	297
28	0.45	1.83	0.65	2.36	1.70	0.70	0.78	1.28	238
Average	N/A	N/A	N/A	N/A	2.13	0.51	0.67	1.49	218

the observed failure load was greater than the predicted failure load. An observation made throughout the testing program was that the compression web members underwent significant out-of-plane deflections as the ultimate load was approached. As discussed above, limiting Equation 12 to a value of 1.0, limits the amount of deflection and axial load the compression web member is subjected to. Recognizing this limit on deflections, column 9 is an attempt to draw an analogy to the deflection limits common in the serviceability requirements of beams. The values in column 8 give the equivalent L/value deflection limit that is applied by limiting the interaction value of Equation 12 to 1.0.

VI. CONCLUSIONS

A. GENERAL

The purpose of this investigation was to develop design recommendations for compression web members in cold-formed steel truss assemblies used in residential roofing applications. Throughout this study, research work has been performed to develop an understanding of the behavior necessary to propose such design recommendations. The research work has included 28 full-scale tests in which the top and bottom chords were over-designed relative to an optimally designed truss assembly. This was done so that the compression web member would be the critical member in the truss assembly. In this section, design recommendations are presented for the design of compression web members in cold-formed steel trusses.

B. MODELING RECOMMENDATIONS

In the modeling of cold-formed steel truss assemblies it is necessary to make several assumptions to keep the analysis from becoming excessively detailed. The results of this study and the work of Harper[2] show that cold-formed steel truss assemblies can be adequately modeled as two-dimensional frame structures. Assumptions made in the modeling of the truss assemblies in this testing program are discussed in Section IV-B.

It is recommended that any connection fabricated by connecting two individual cold-formed steel sections together using self-drilling screws be modeled as a pin connection. On the other hand, a member such as a chord member that is fabricated

from a single section that supported by more than two joints could appropriately be modeled as continuous through the interior joints. However, the ends of the continuous member which do not run continuously through a joint should not be considered able to transfer moments.

When modeling the cold-formed steel truss assemblies as two-dimensional frame structures it is important to recognize that the computer model is not capable of considering connection eccentricities. When interpreting the output from such a model it is imperative that the designer recognize that such eccentricities exist and can cause additional moments to act on the structure.

C. DESIGN RECOMMENDATIONS

The recommendations given in this section are valid for the design of compression web members in cold-formed steel truss assemblies in which the chords are over-designed relative to an optimally designed truss assembly.

1. Nominal Axial Capacity. The Nominal Axial Capacity, P_n, of a compression web member shall be determined in accordance with Section C4 of the AISI Specification[3]. As discussed in Section V-E, the controlling behavior of the compression web members was observed to be flexural buckling about the weak-axis. This is due to the eccentric nature of the load application when the connection of the C-sections is made with the C-sections in a back-to-back configuration. The eccentric load application causes the compression web member to bend about its minor-axis. The minor-axis bending behavior does not produce shear flows that would cause twisting of the section. Because of this and the rotational restraint provided by the back-to-back

C-Section connection, torsional-flexural buckling is not a possible failure mode in this situation. Therefore, it is recommended that the capacity of the compression web members be calculated using the AISI Specification but recognizing that the back-to-back connection of C-sections inhibits torsional-flexural buckling. This recommendation is valid for compression web members with L/r greater than 100.

2. Interaction Equation. As discussed in Section V, the compression web members in cold-formed steel truss assemblies were observed to behave as beam-columns. The AISI Specification[3] requires beam-columns to meet the conditions of Interaction Equations C5-1 and C5-2, shown as Equations 4 and 5 in Section II-D.2 of this document. As discussed in Section V-E, Equation 4 is the appropriate interaction equation to consider for the condition of stability away from the supports being the controlling behavior. To calculate the interaction values for the experimental results, Equation 4 was modified by removing the factors of safety to obtain Equation 12. As shown in column 5 of Table V, the results of this experimental study show that interaction values greater than 1.0 were obtainable. The interaction values at the observed failure loads ranged from 1.53 to 3.24 with an average value of 2.13. Recognizing the scatter in the interaction values computed at the observed failure loads, it is recommended that a lower bound value of 1.5 may be used to provide a safe design for compression web members which meet the conditions of this section.

However, to remain consistent with the form of the AISI Specification[3] such that the right hand side of the interaction equation is held at 1.0, an alternative approach is proposed. It is recommended that the conditions of interaction equation C5-1 of the AISI Specification, Equation 4 in this document, be met in the design of compression web

members of cold-formed steel truss assemblies with the following modification being made. The applied axial load, P, predicted by the computer model may be reduced by a ratio to be determined from the test results. As shown in column 7 of Table V, the ratio of the values of the axial load carried by the compression web member at the predicted failure load to the value at the observed failure load ranged from 0.50 to 0.79 with an average value of 0.67. Again, to recognize the scatter in these ratios, it is recommended that an upper bound value of 0.80 may be chosen. Therefore, based upon the results of this experimental program, it is recommended that the following conditions should be met for the design of compression web members that meet the conditions of this section. The axial force shall satisfy the interaction equation shown as Equation 13.

$$\frac{P'}{P_a} + \frac{C_{my} M_y}{M_{ay} \alpha_y} \leq 1.0 \qquad (13)$$

where $P' = 0.80(P)$

P = Axial force in compression web as predicted by computer model

P_a = Allowable axial capacity computed using Section VI-C.1

$M_y = P'(e)$

M_{ay} = Allowable moment about the minor axis

$1/\alpha_y = 1/[1-(\Omega_c P'/P_{cr})]$, Magnification factor

e = Distance from the outside of the web to the centroid of the section

P_{cr} = Elastic buckling strength about axis of bending

C_{my} = End moment coefficient for y axis

The design recommendations given in this section are valid only for compression web members in cold-formed steel truss assemblies that meet the following requirements that describe the range of parameters of the testing program. Using an effective length factor of unity, the slenderness ratio of the compression web member must be between 100 and 180. The base metal thickness of the compression web members must be between 0.036 inches and 0.059 inches. As described in Section III-C, the truss assemblies tested in this experimental program were designed such that the compression web member would be the weakest structural element in the assembly. Because of this, the design recommendations are valid only for truss assemblies in which the compression web member controls the design of the assembly. The top flange of the top chord of the truss assembly must be restrained against out-of-plane movement along the length of the top chord. The bottom flange of the top chord must be restrained against out-of-plane movement at intervals of no greater than 36 inches.

Alternatively, if transverse deflections are a concern in the structure being designed, the designer should choose to use the full axial force, P, in the compression member in evaluating the interaction equation in Equation 13. As discussed in Section V-E, limiting the interaction equation to a value of 1.0, limits the amount of deflection and axial load that the compression web member is subjected to. The equivalent deflection limit that is derived from this limit on the interaction equation is approximately L/200.

VII. FUTURE RESEARCH

Throughout this testing program it has become evident that the stiffness of the chords compared to that of the compression web member can significantly affect the behavior of the compression web member. The stiffness of the top chord is particularly critical. The stiffness of the top chord is affected not only by its geometry, but also the amount of bracing that is provided to preclude out-of-plane movement. The top chord must be adequately braced to prevent out-of-plane rotation that can significantly increase the level of deflections that occur in the compression web member. This testing program has only considered truss assemblies in which the top chord was over-designed relative to an optimally designed truss assembly. More research is necessary to determine the behavior of the compression web members in truss assemblies that have been optimally designed.

APPENDIX A.

DETAILED DRAWINGS OF TRUSS ASSEMBLIES

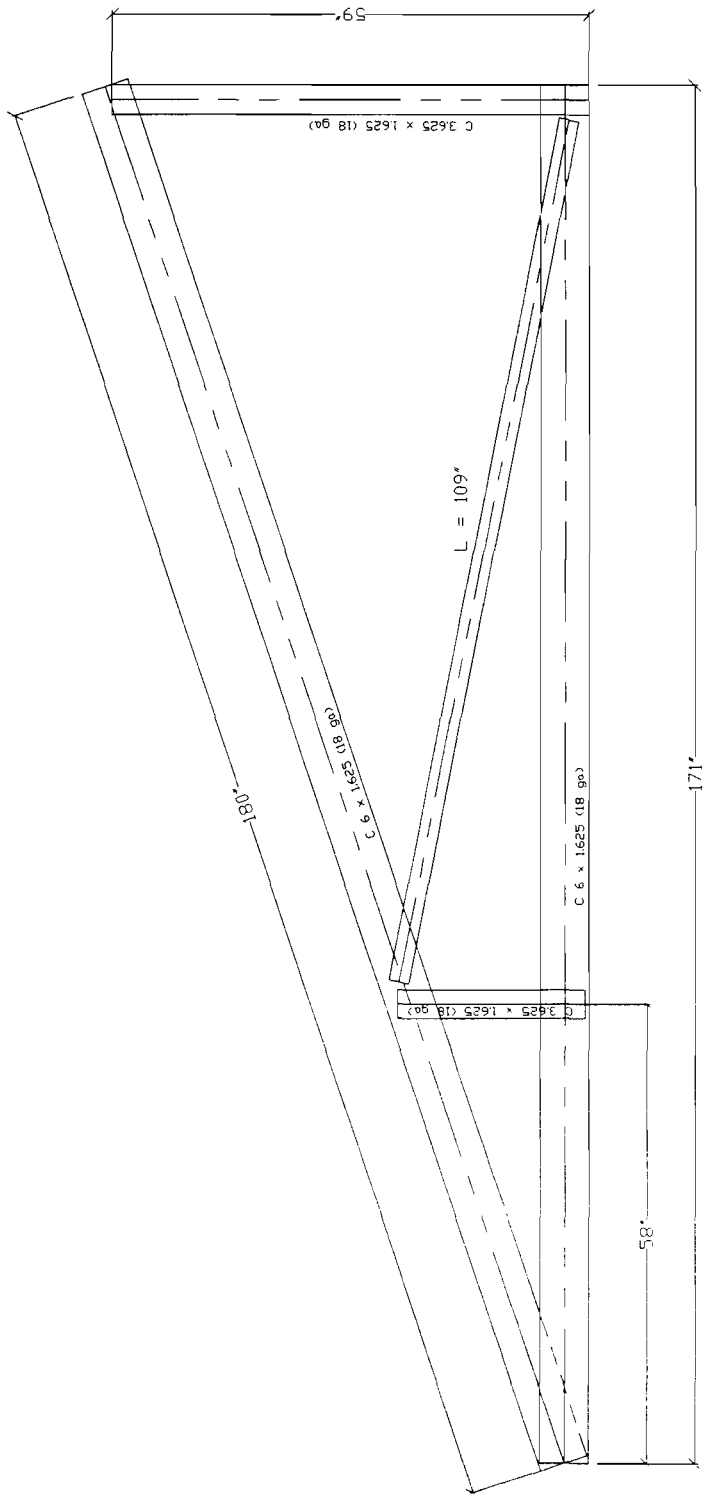
59"
C 3.625 x 1.625 (18 ga)
L = 109"
180"
C 6 x 1.625 (18 ga)
171"
C 6 x 1.625 (18 ga)
C 3.625 x 1.625 (18 ga)
58"

Tests 1 - 7

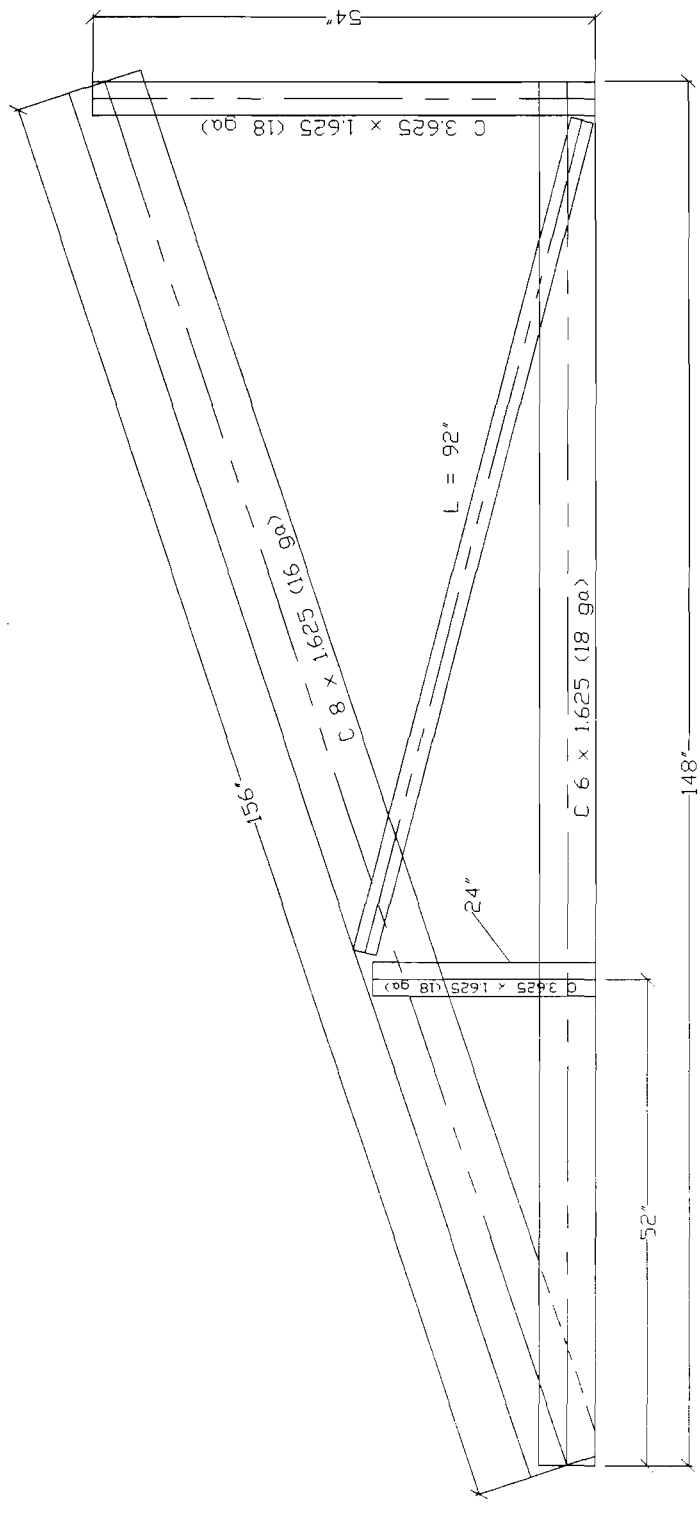
54"
C 3.625 x 1.625 (18 ga)
L = 92"
C 8 x 1.625 (16 ga)
C 6 x 1.625 (18 ga)
156"
148"
24"
C 3625 x 1.625 (18 ga)
52"

Tests 8 - 13

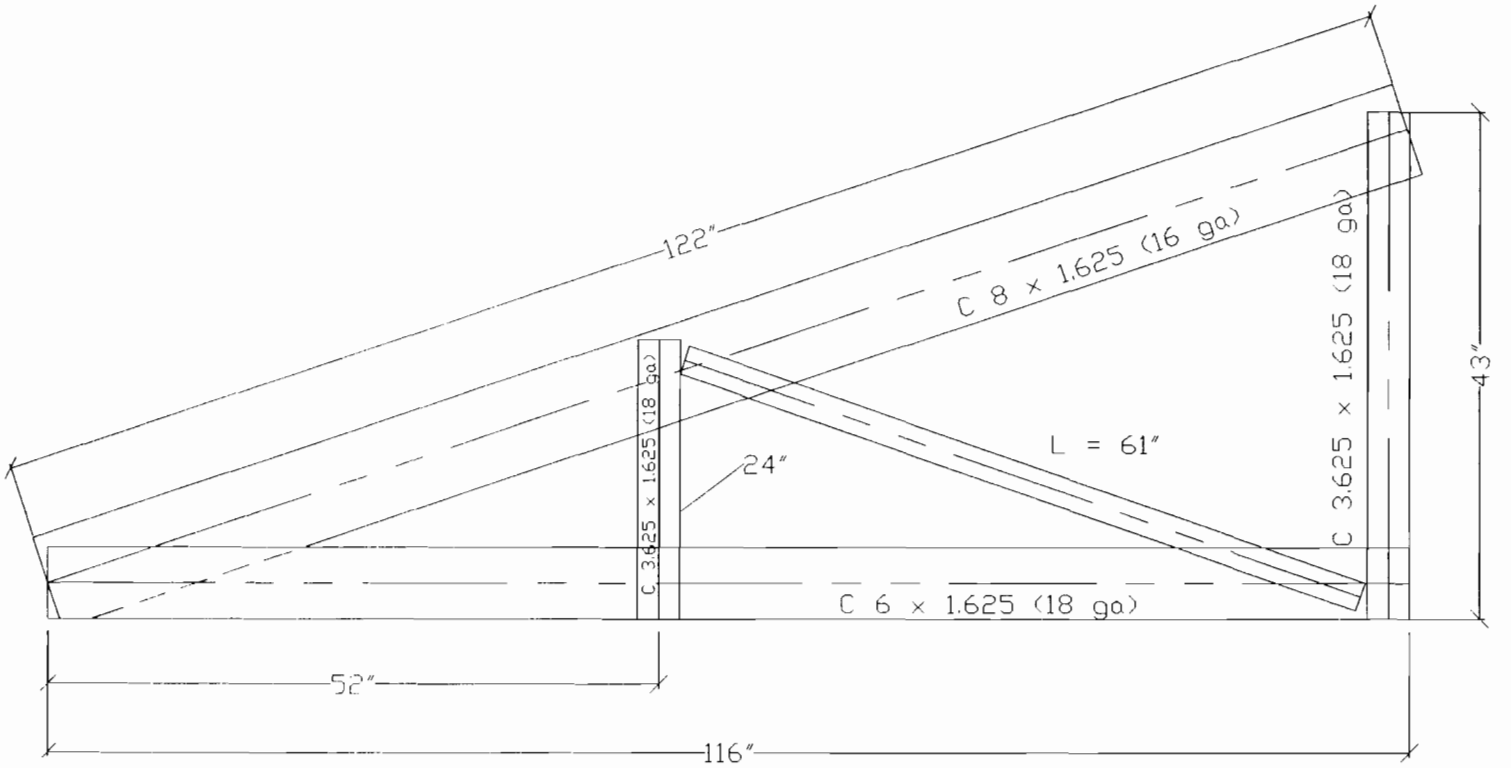
122"
C 8 x 1.625 (16 ga)
C 3.625 x 1.625 (18 ga)
C 3.625 x 1.625 (18 ga)
43"
L = 61"
24"
C 6 x 1.625 (18 ga)
52"
116"

Tests 14 - 19

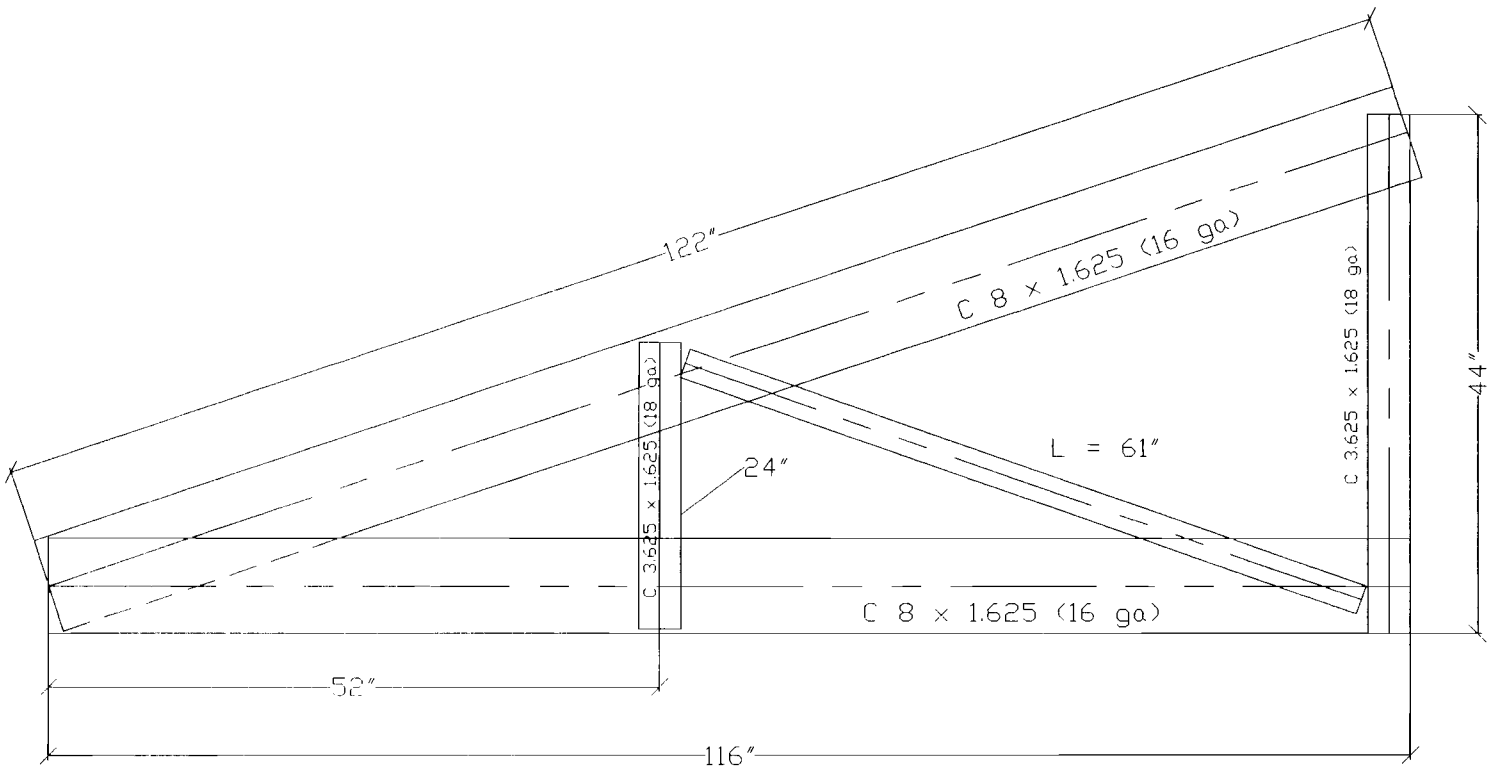
122"
C 8 x 1.625 (16 ga)
C 3.625 x 1.625 (18 ga)
44"
L = 61"
24"
C 3.625 x 1.625 (18 ga)
C 8 x 1.625 (16 ga)
52"
116"

Tests 20 - 22

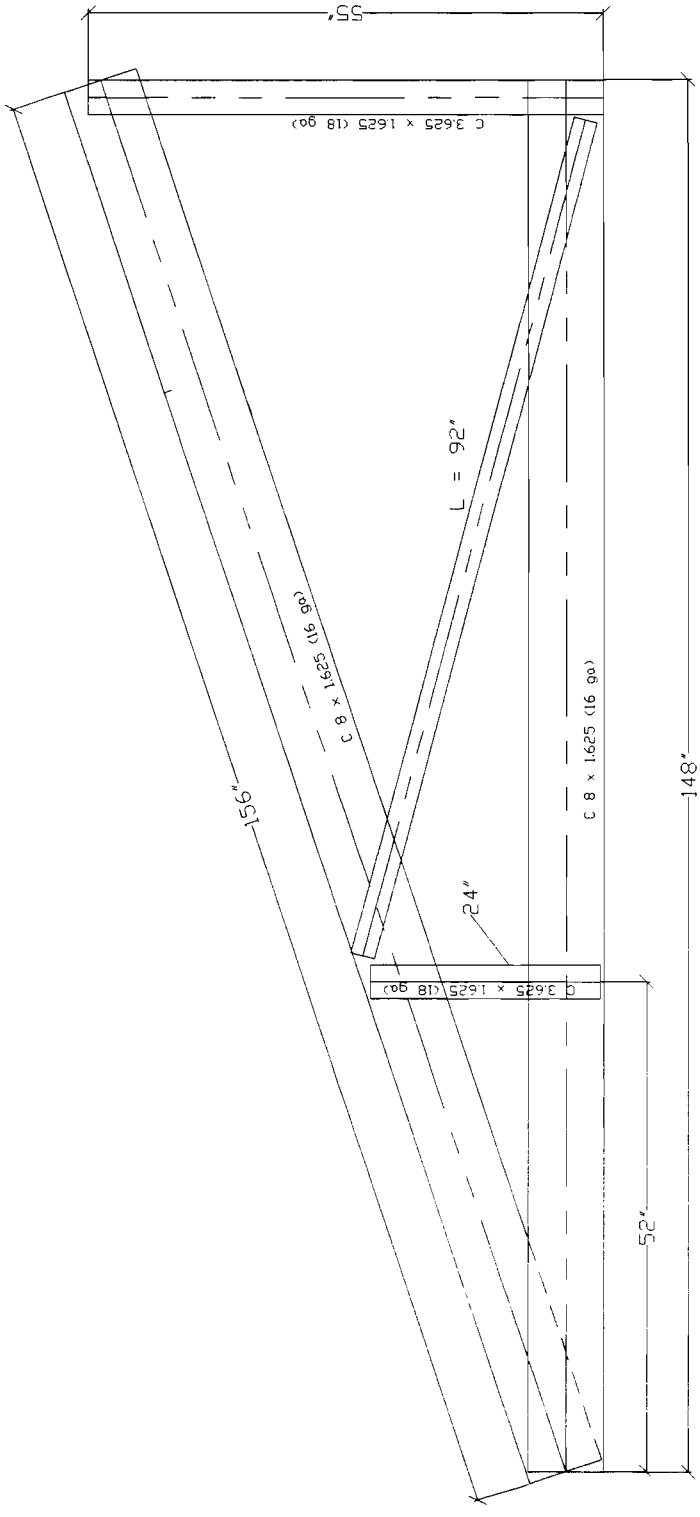
55"
C 3.625 x 1.625 (18 ga)
L = 92"
C 8 x 1.625 (16 ga)
156"
C 8 x 1.625 (16 ga)
148"
24"
C 3.625 x 1.625 (18 ga)
52"

Tests 23 - 25

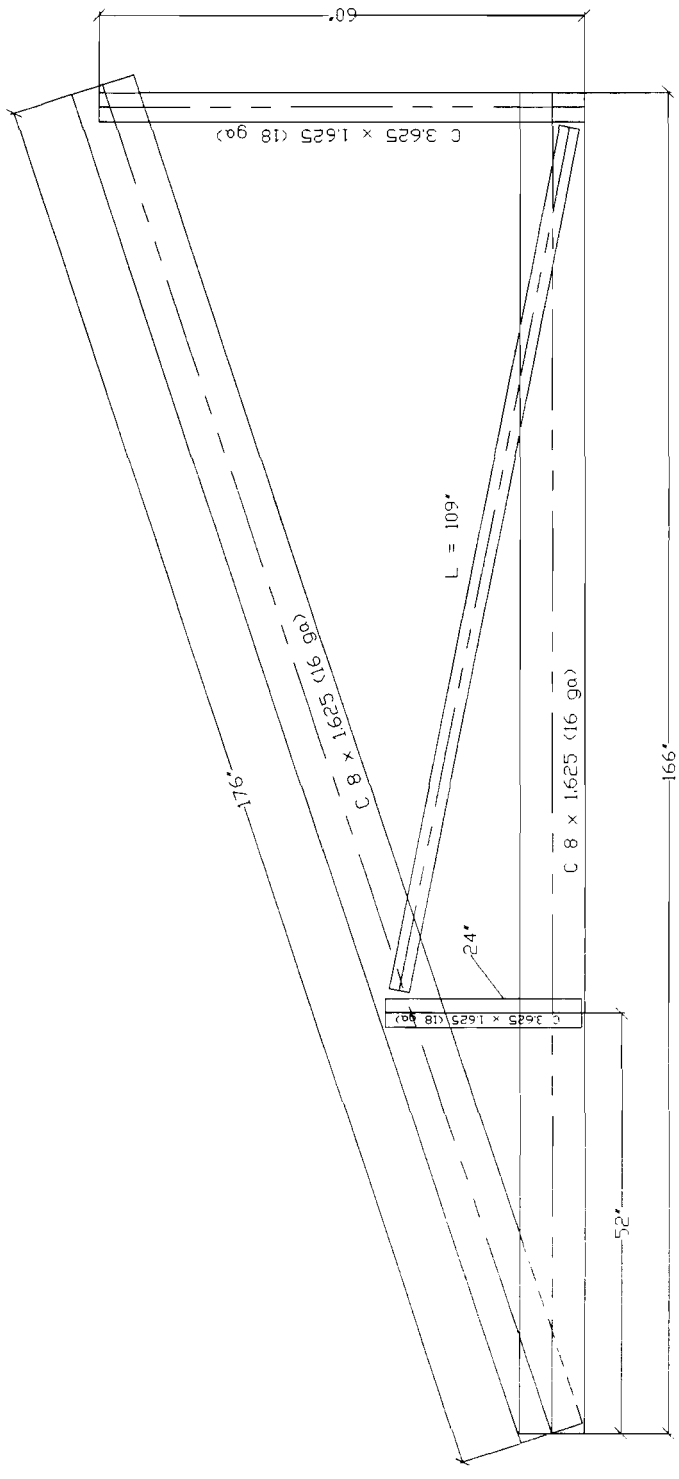
60"
C 3.625 x 1.625 (18 ga)
L = 109"
C 8 x 1.625 (16 ga)
176"
C 8 x 1.625 (16 ga)
24"
C 3.625 x 1.625 (18 ga)
166"
52"

Tests 26 - 28

APPENDIX B.

PLOTS OF COMPRESSIVE STRESS VS. TOTAL LOAD ON TRUSS ASSEMBLY

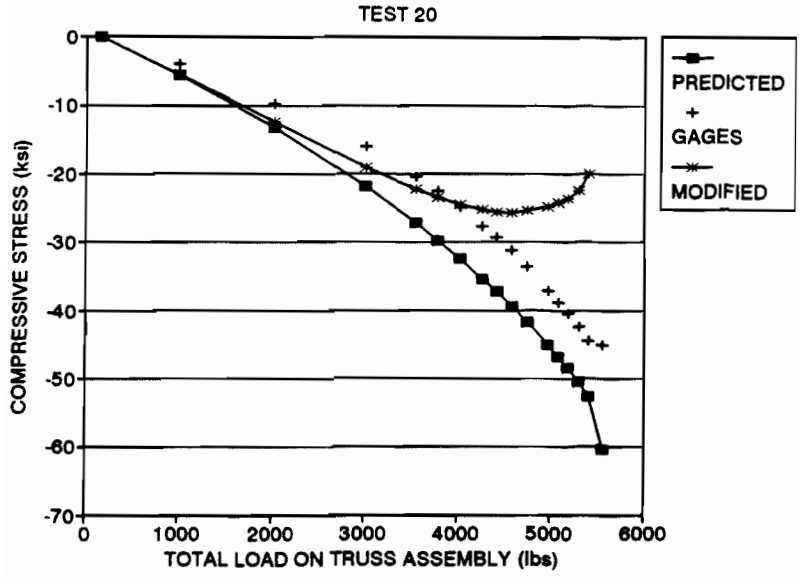
TEST 20
COMPRESSIVE STRESS (ksi)
0
-10
-20
-30
-40
-50
-60
-70
0
1000
2000
3000
4000
5000
6000
TOTAL LOAD ON TRUSS ASSEMBLY (lbs)
PREDICTED
GAGES
MODIFIED

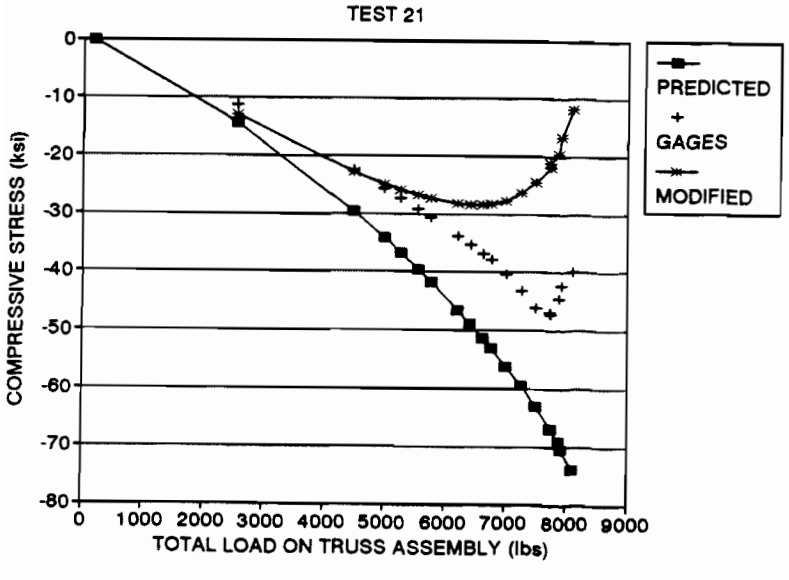
TEST 21
COMPRESSIVE STRESS (ksi)
0
-10
-20
-30
-40
-50
-60
-70
-80
0
1000
2000
3000
4000
5000
6000
7000
8000
9000
TOTAL LOAD ON TRUSS ASSEMBLY (lbs)
PREDICTED
GAGES
MODIFIED

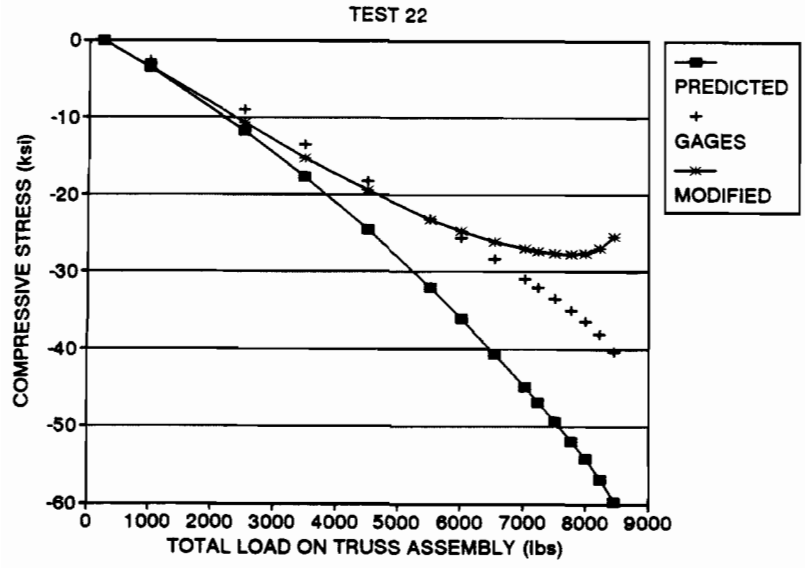
TEST 22
COMPRESSIVE STRESS (ksi)
0
-10
-20
-30
-40
-50
-60
0
1000
2000
3000
4000
5000
6000
7000
8000
9000
TOTAL LOAD ON TRUSS ASSEMBLY (lbs)
PREDICTED
GAGES
MODIFIED

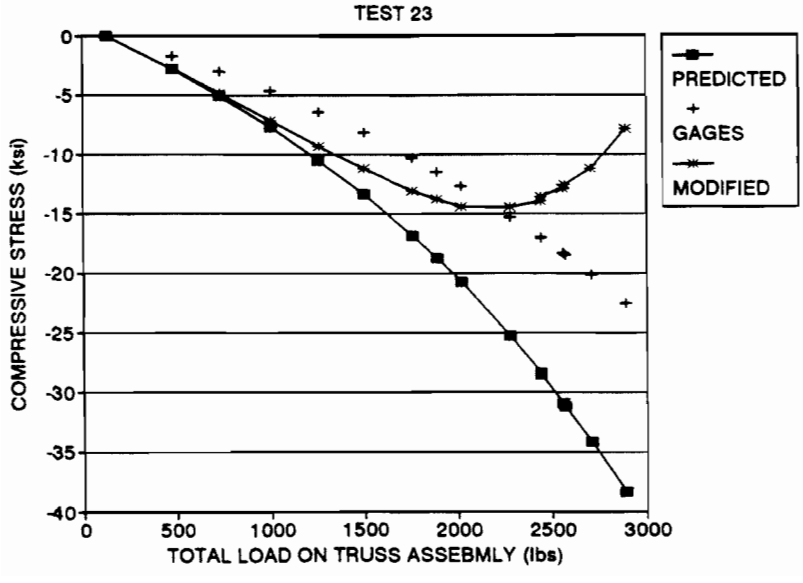
TEST 23
COMPRESSIVE STRESS (ksi)
0
-5
-10
-15
-20
-25
-30
-35
-40
0
500
1000
1500
2000
2500
3000
TOTAL LOAD ON TRUSS ASSEBMLY (lbs)
PREDICTED
GAGES
MODIFIED

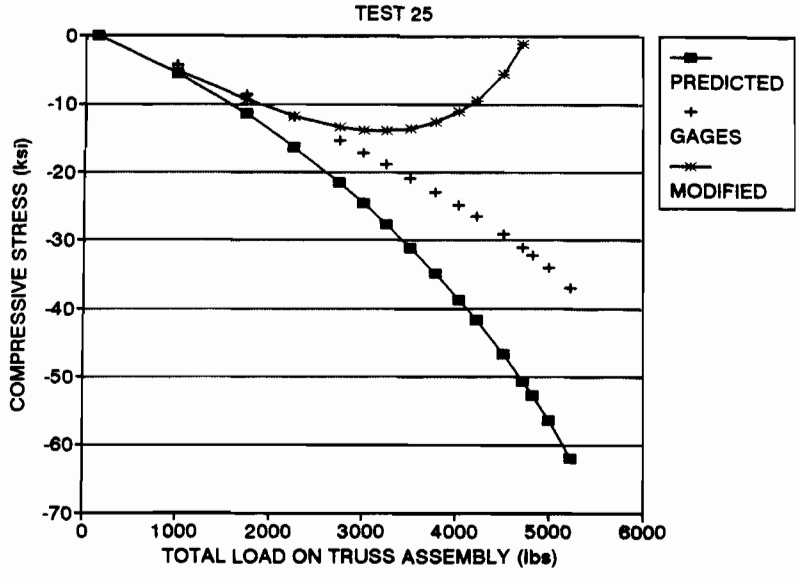
TEST 25
COMPRESSIVE STRESS (ksi)
0
-10
-20
-30
-40
-50
-60
-70
0
1000
2000
3000
4000
5000
6000
TOTAL LOAD ON TRUSS ASSEMBLY (lbs)
PREDICTED
GAGES
MODIFIED

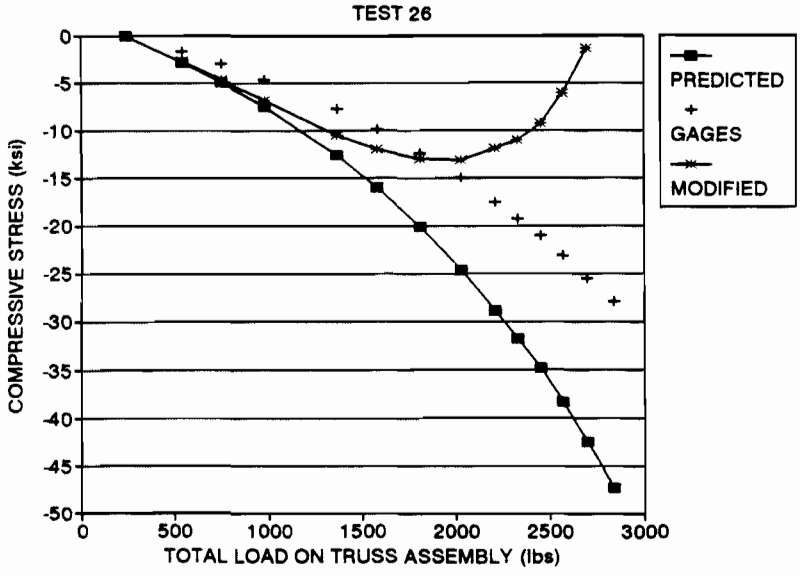
TEST 26
COMPRESSIVE STRESS (ksi)
0
-5
-10
-15
-20
-25
-30
-35
-40
-45
-50
0
500
1000
1500
2000
2500
3000
TOTAL LOAD ON TRUSS ASSEMBLY (lbs)
PREDICTED
GAGES
MODIFIED

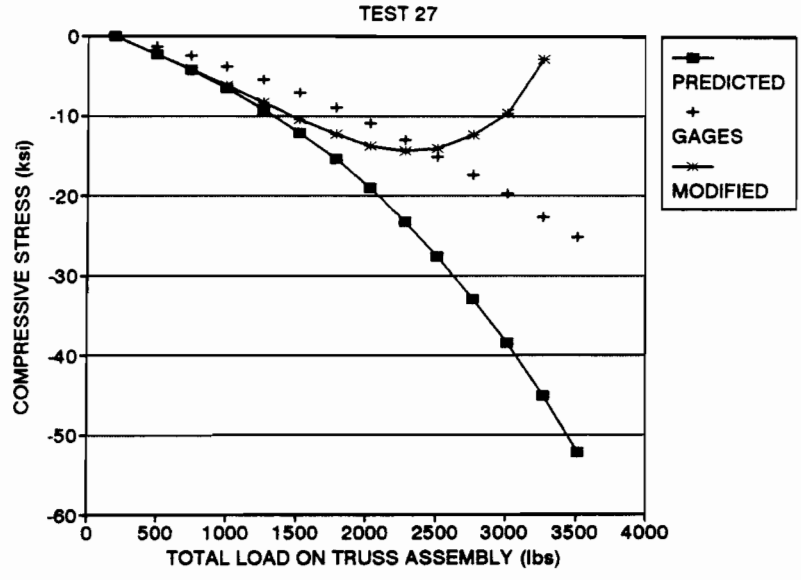
TEST 27
COMPRESSIVE STRESS (ksi)
0
-10
-20
-30
-40
-50
-60
0
500
1000
1500
2000
2500
3000
3500
4000
TOTAL LOAD ON TRUSS ASSEMBLY (lbs)
PREDICTED
GAGES
MODIFIED

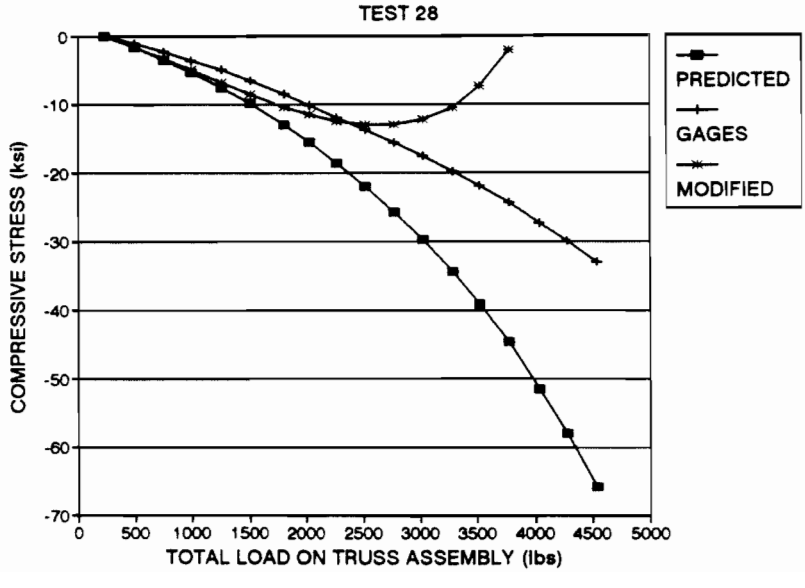
TEST 28
COMPRESSIVE STRESS (ksi)
0
-10
-20
-30
-40
-50
-60
-70
0
500
1000
1500
2000
2500
3000
3500
4000
4500
5000
TOTAL LOAD ON TRUSS ASSEMBLY (lbs)
PREDICTED
GAGES
MODIFIED

APPENDIX C.

PLOTS OF DEFLECTION VS. TOTAL LOAD ON TRUSS ASSEMBLY

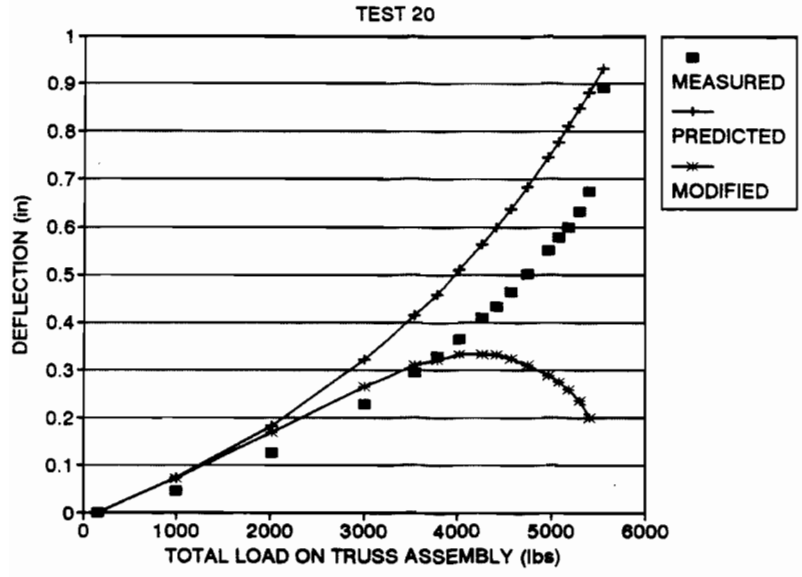
TEST 20
DEFLECTION (in)
TOTAL LOAD ON TRUSS ASSEMBLY (lbs)
MEASURED
PREDICTED
MODIFIED
0
0.1
0.2
0.3
0.4
0.5
0.6
0.7
0.8
0.9
1
0
1000
2000
3000
4000
5000
6000

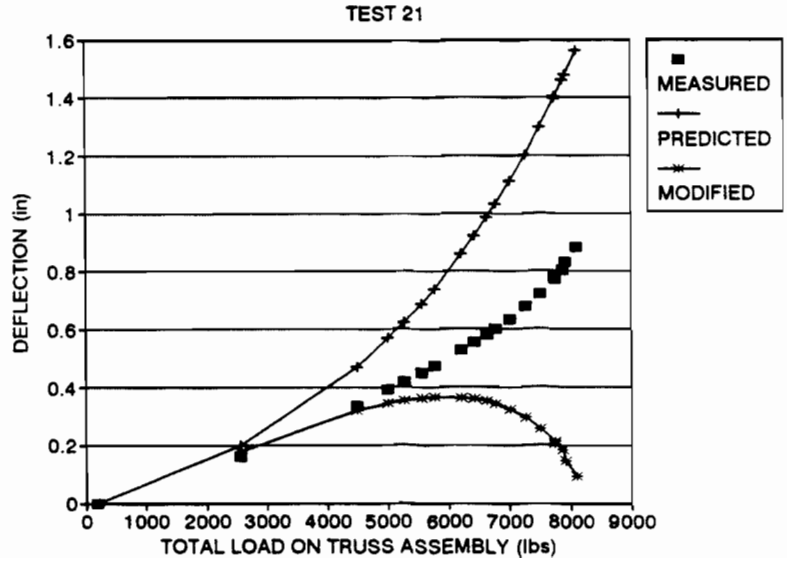
TEST 21
DEFLECTION (in)
TOTAL LOAD ON TRUSS ASSEMBLY (lbs)
MEASURED
PREDICTED
MODIFIED
0
0.2
0.4
0.6
0.8
1
1.2
1.4
1.6
0
1000
2000
3000
4000
5000
6000
7000
8000
9000

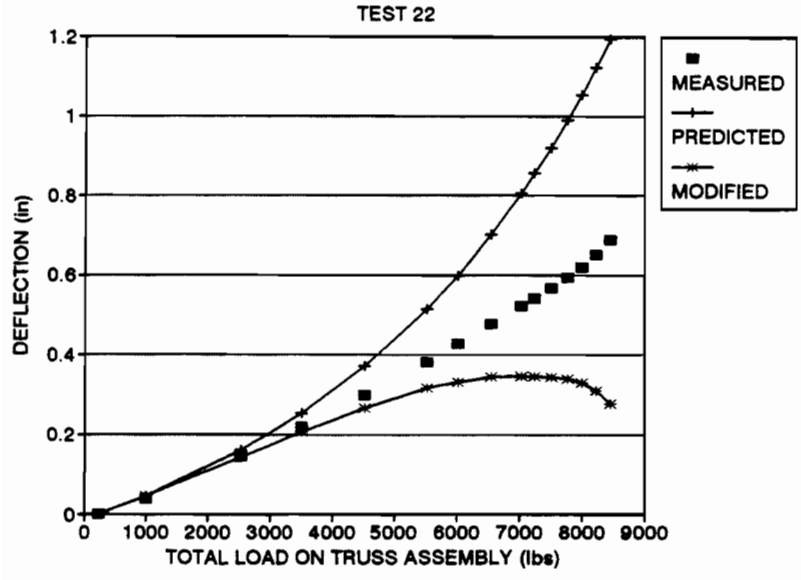
TEST 22
DEFLECTION (in)
1.2
1
0.8
0.6
0.4
0.2
0
0 1000 2000 3000 4000 5000 6000 7000 8000 9000
TOTAL LOAD ON TRUSS ASSEMBLY (lbs)
MEASURED
PREDICTED
MODIFIED

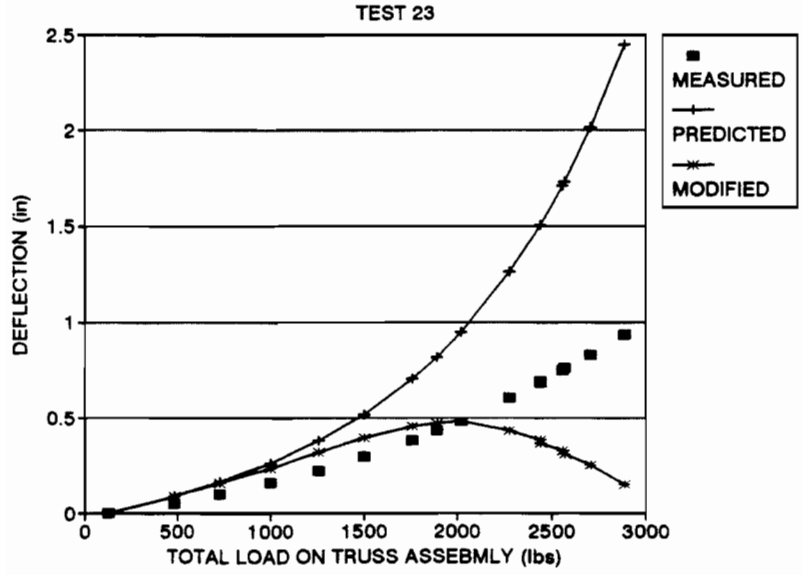
TEST 23
DEFLECTION (in)
2.5
2
1.5
1
0.5
0
0 500 1000 1500 2000 2500 3000
TOTAL LOAD ON TRUSS ASSEBMLY (lbs)
MEASURED
PREDICTED
MODIFIED

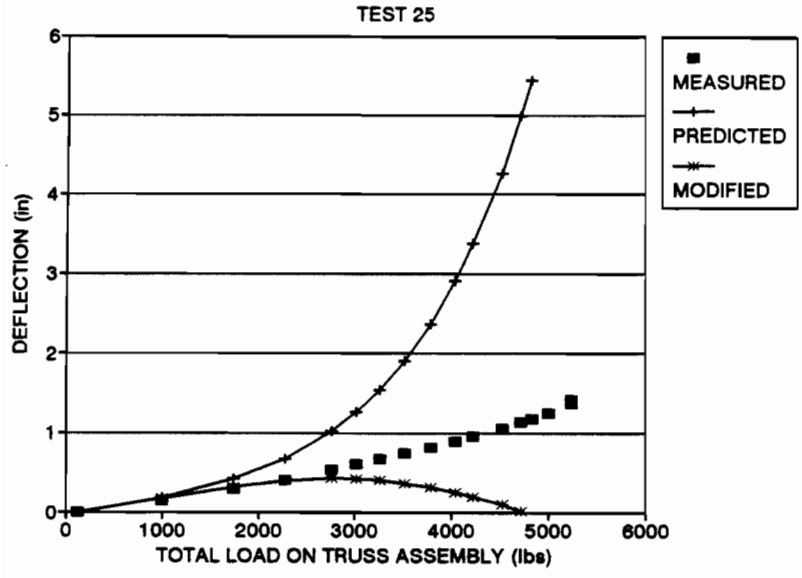
TEST 25
DEFLECTION (in)
TOTAL LOAD ON TRUSS ASSEMBLY (lbs)
MEASURED
PREDICTED
MODIFIED
0
1
2
3
4
5
6
0
1000
2000
3000
4000
5000
6000

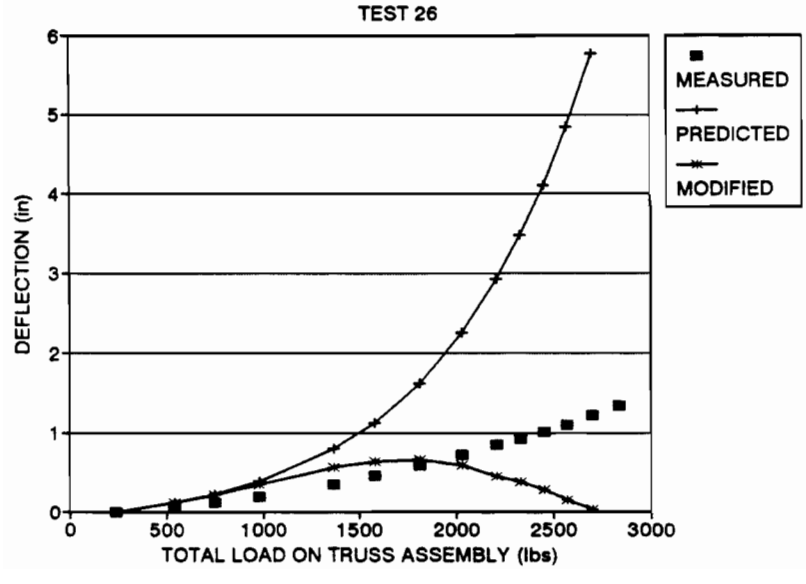
TEST 26
DEFLECTION (in)
TOTAL LOAD ON TRUSS ASSEMBLY (lbs)
MEASURED
PREDICTED
MODIFIED
0
1
2
3
4
5
6
0
500
1000
1500
2000
2500
3000

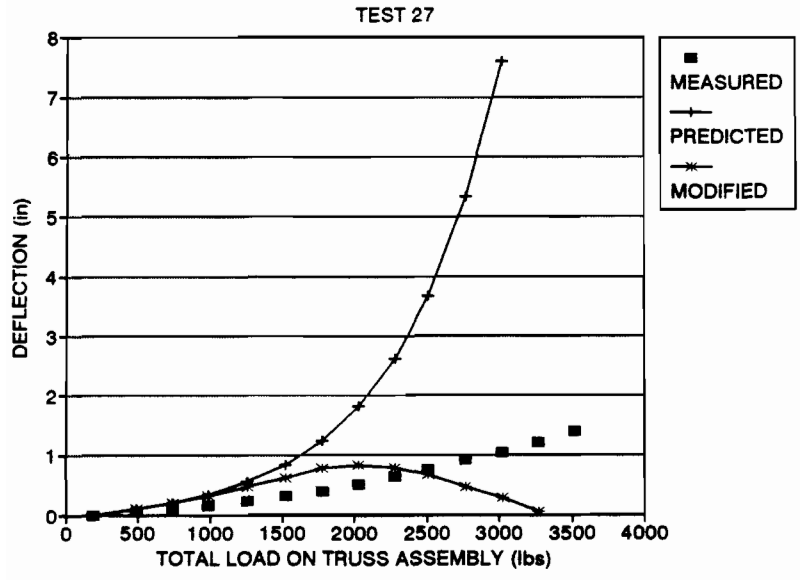
TEST 27
DEFLECTION (in)
0
1
2
3
4
5
6
7
8
0
500
1000
1500
2000
2500
3000
3500
4000
TOTAL LOAD ON TRUSS ASSEMBLY (lbs)
MEASURED
PREDICTED
MODIFIED

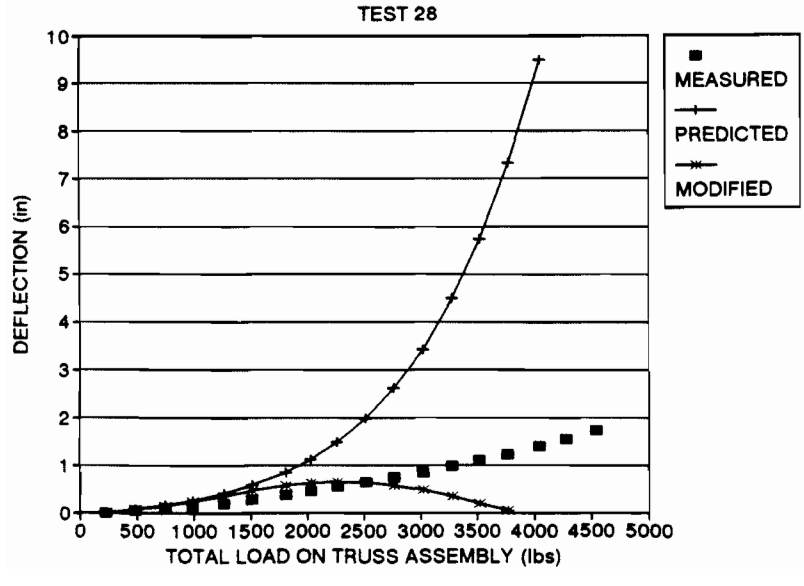
TEST 28
DEFLECTION (in)
0
1
2
3
4
5
6
7
8
9
10
0
500
1000
1500
2000
2500
3000
3500
4000
4500
5000
TOTAL LOAD ON TRUSS ASSEMBLY (lbs)
MEASURED
PREDICTED
MODIFIED

APPENDIX D.

PLOTS OF AXIAL LOAD VS. TOTAL LOAD ON TRUSS ASSEMBLY

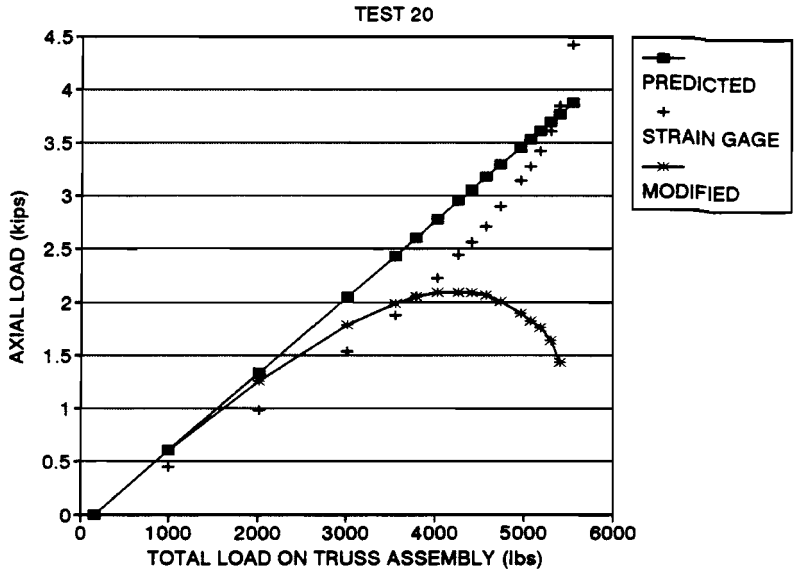
TEST 20
AXIAL LOAD (kips)
4.5
4
3.5
3
2.5
2
1.5
1
0.5
0
0
1000
2000
3000
4000
5000
6000
TOTAL LOAD ON TRUSS ASSEMBLY (lbs)
PREDICTED
STRAIN GAGE
MODIFIED

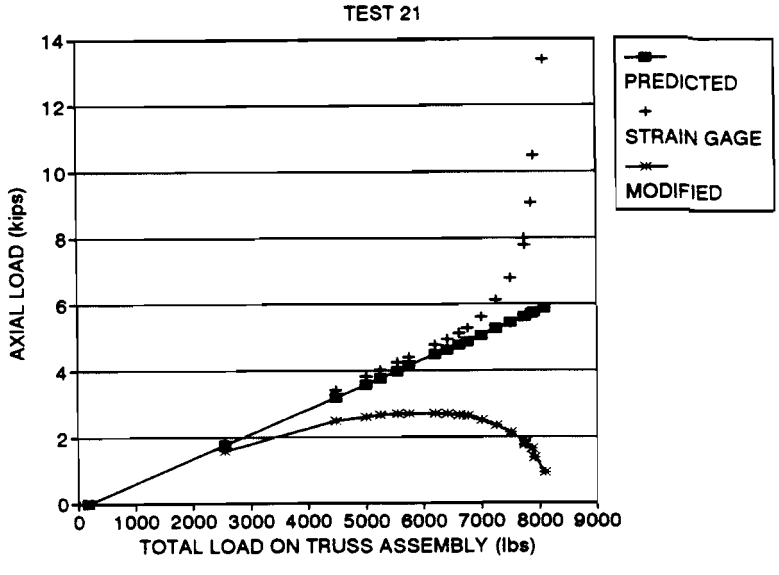
TEST 21
AXIAL LOAD (kips)
14
12
10
8
6
4
2
0
0 1000 2000 3000 4000 5000 6000 7000 8000 9000
TOTAL LOAD ON TRUSS ASSEMBLY (lbs)
PREDICTED
STRAIN GAGE
MODIFIED

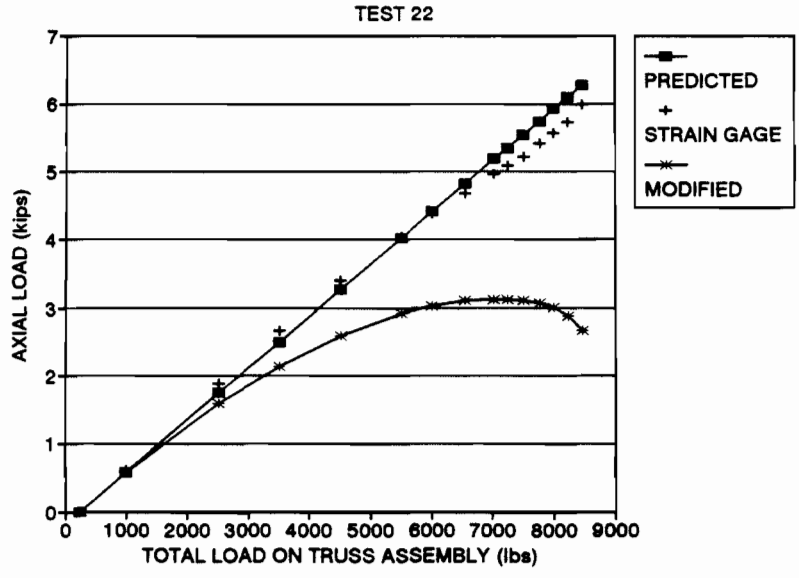
TEST 22
AXIAL LOAD (kips)
0
1
2
3
4
5
6
7
0 1000 2000 3000 4000 5000 6000 7000 8000 9000
TOTAL LOAD ON TRUSS ASSEMBLY (lbs)
PREDICTED
STRAIN GAGE
MODIFIED

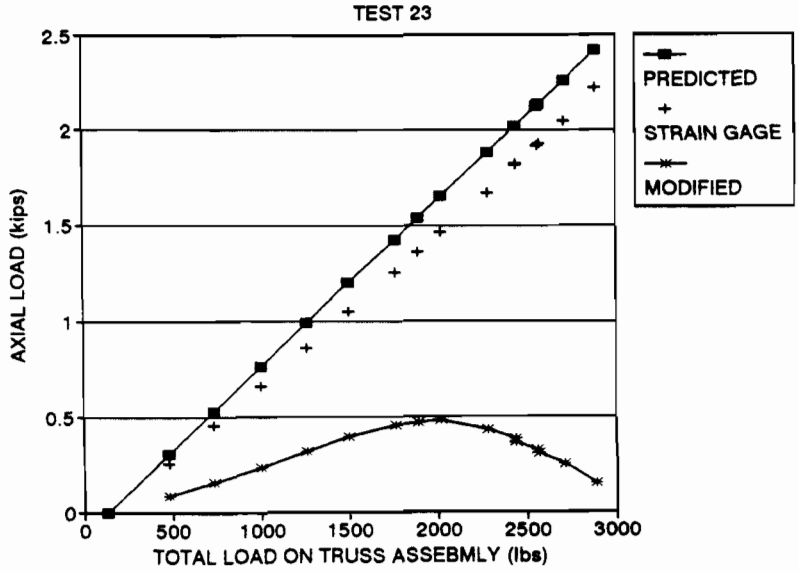
TEST 23
AXIAL LOAD (kips)
0
0.5
1
1.5
2
2.5
0 500 1000 1500 2000 2500 3000
TOTAL LOAD ON TRUSS ASSEBMLY (lbs)
PREDICTED
STRAIN GAGE
MODIFIED

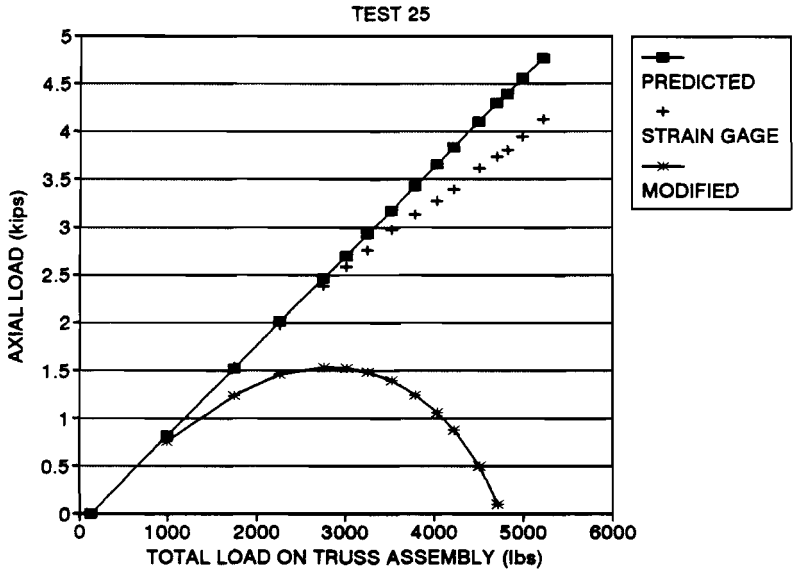
TEST 25
AXIAL LOAD (kips)
5
4.5
4
3.5
3
2.5
2
1.5
1
0.5
0
0
1000
2000
3000
4000
5000
6000
TOTAL LOAD ON TRUSS ASSEMBLY (lbs)
PREDICTED
STRAIN GAGE
MODIFIED

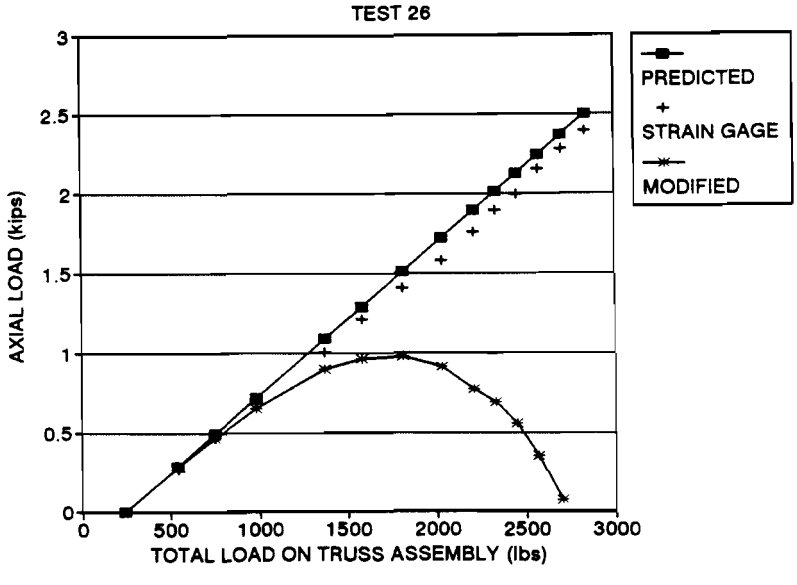
TEST 26
AXIAL LOAD (kips)
3
2.5
2
1.5
1
0.5
0
0
500
1000
1500
2000
2500
3000
TOTAL LOAD ON TRUSS ASSEMBLY (lbs)
PREDICTED
STRAIN GAGE
MODIFIED

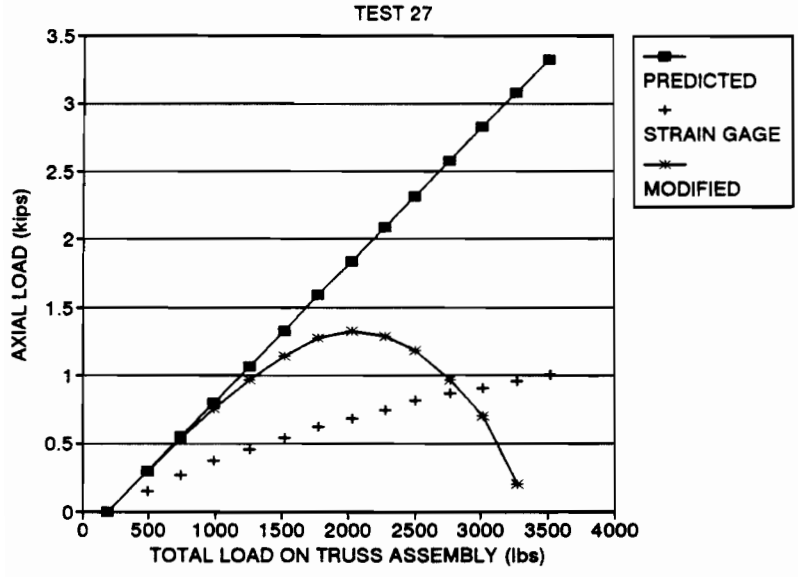
TEST 27
AXIAL LOAD (kips)
TOTAL LOAD ON TRUSS ASSEMBLY (lbs)
PREDICTED
STRAIN GAGE
MODIFIED
0
0.5
1
1.5
2
2.5
3
3.5
0
500
1000
1500
2000
2500
3000
3500
4000

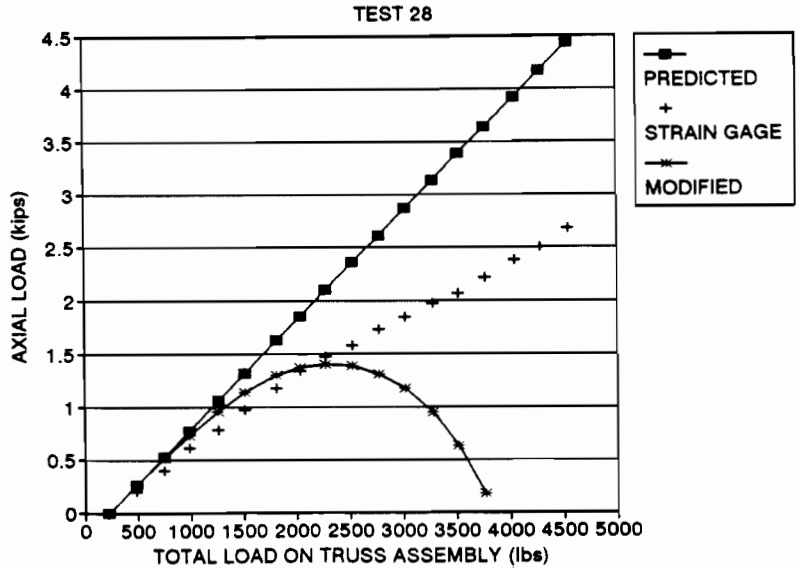
TEST 28
AXIAL LOAD (kips)
TOTAL LOAD ON TRUSS ASSEMBLY (lbs)
PREDICTED
STRAIN GAGE
MODIFIED
0
0.5
1
1.5
2
2.5
3
3.5
4
4.5
0
500
1000
1500
2000
2500
3000
3500
4000
4500
5000

APPENDIX E.

PLOTS OF RESTRAINT MOMENTS VS. TOTAL LOAD ON TRUSS ASSEMBLY

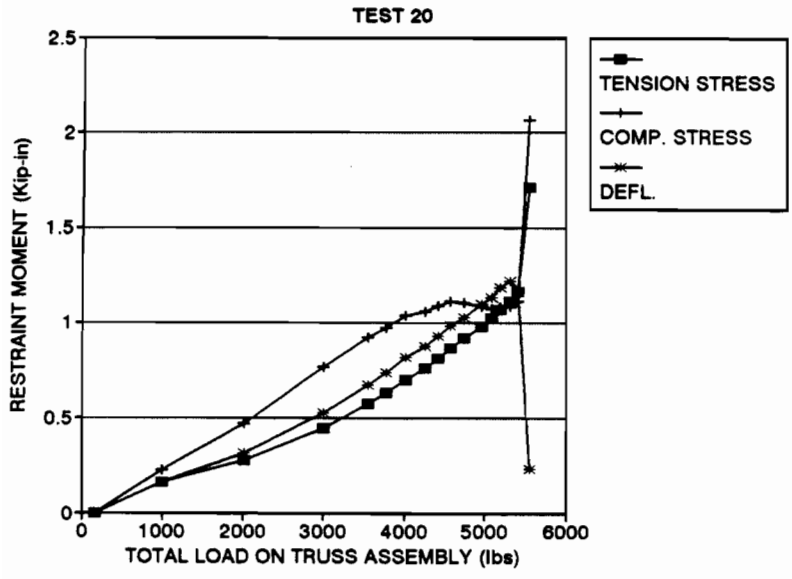
TEST 20
RESTRAINT MOMENT (Kip-in)
2.5
2
1.5
1
0.5
0
0
1000
2000
3000
4000
5000
6000
TOTAL LOAD ON TRUSS ASSEMBLY (lbs)
TENSION STRESS
COMP. STRESS
DEFL.

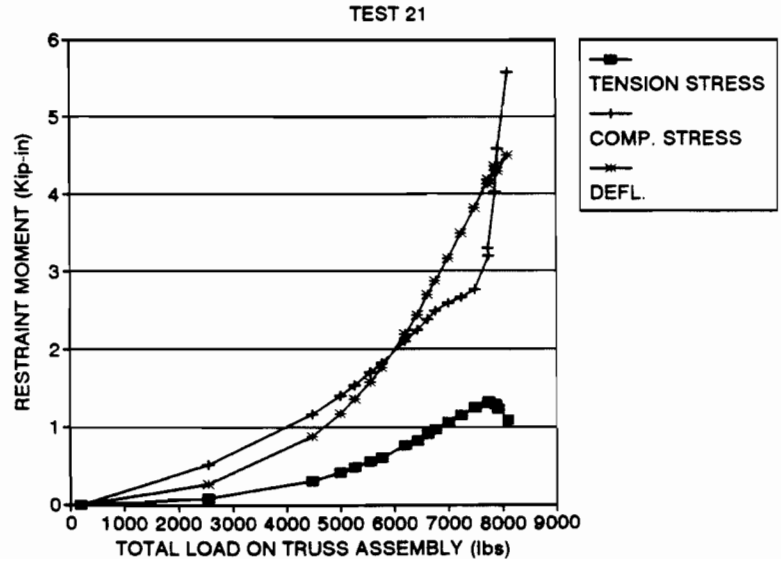
TEST 21
RESTRAINT MOMENT (Kip-in)
6
5
4
3
2
1
0
0 1000 2000 3000 4000 5000 6000 7000 8000 9000
TOTAL LOAD ON TRUSS ASSEMBLY (lbs)
TENSION STRESS
COMP. STRESS
DEFL.

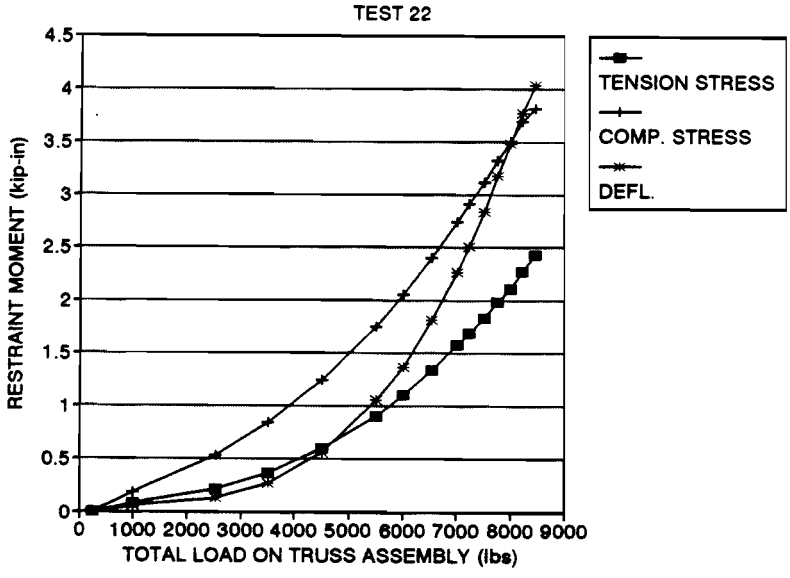
TEST 22
RESTRAINT MOMENT (kip-in)
4.5
4
3.5
3
2.5
2
1.5
1
0.5
0
0 1000 2000 3000 4000 5000 6000 7000 8000 9000
TOTAL LOAD ON TRUSS ASSEMBLY (lbs)
TENSION STRESS
COMP. STRESS
DEFL.

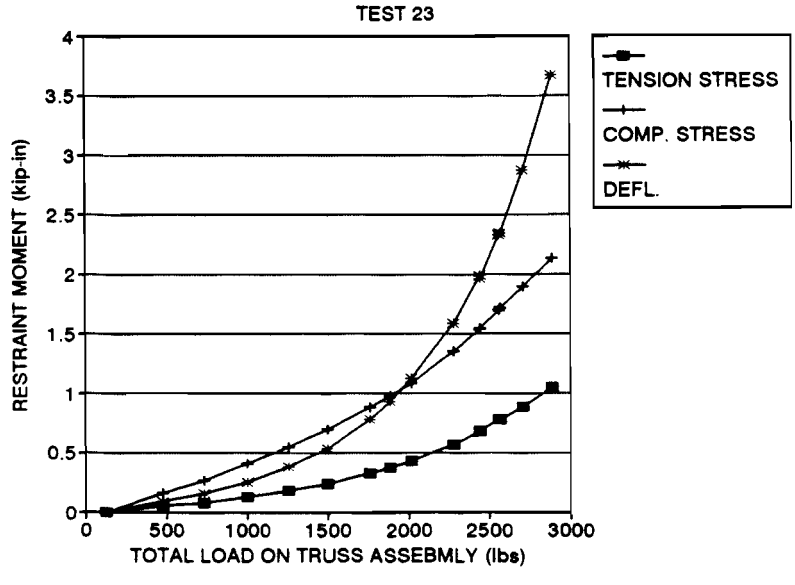
TEST 23
RESTRAINT MOMENT (kip-in)
4
3.5
3
2.5
2
1.5
1
0.5
0
0 500 1000 1500 2000 2500 3000
TOTAL LOAD ON TRUSS ASSEBMLY (lbs)
TENSION STRESS
COMP. STRESS
DEFL.

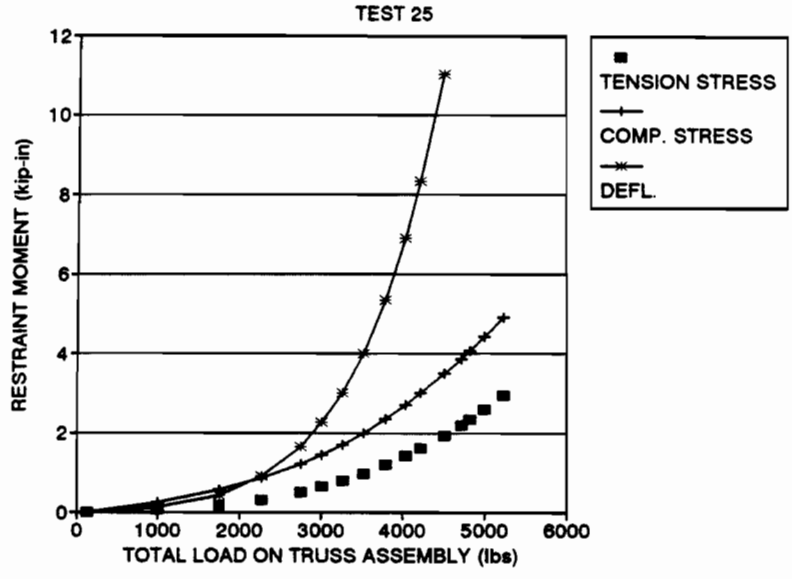
TEST 25
RESTRAINT MOMENT (kip-in)
TOTAL LOAD ON TRUSS ASSEMBLY (lbs)
TENSION STRESS
COMP. STRESS
DEFL.
0
2
4
6
8
10
12
0
1000
2000
3000
4000
5000
6000

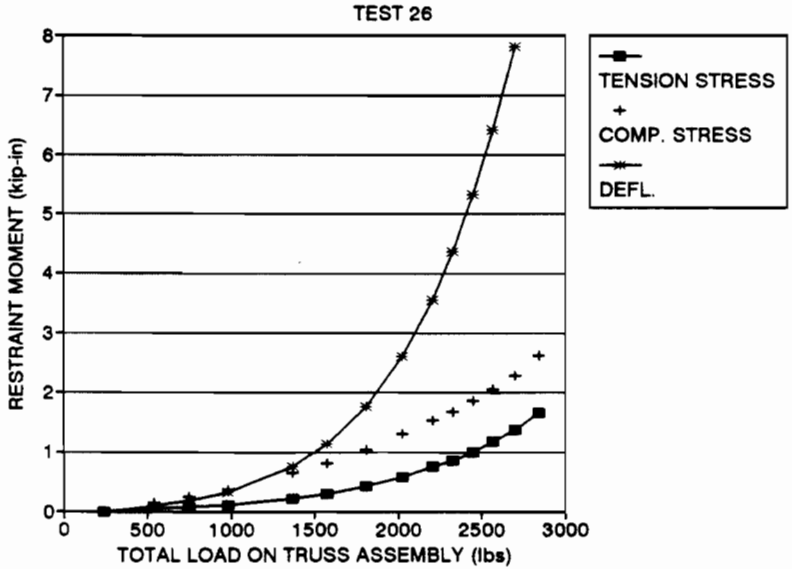
TEST 26
RESTRAINT MOMENT (kip-in)
TOTAL LOAD ON TRUSS ASSEMBLY (lbs)
TENSION STRESS
COMP. STRESS
DEFL.
0
1
2
3
4
5
6
7
8
0
500
1000
1500
2000
2500
3000

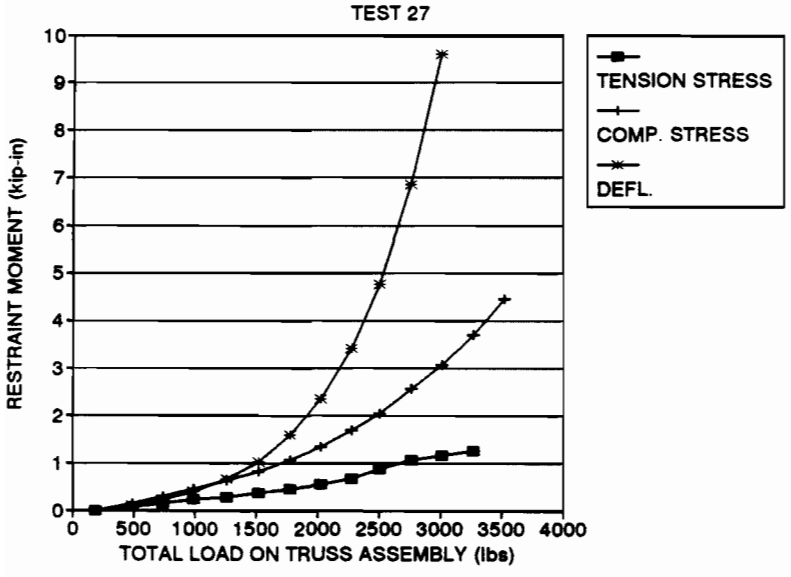
TEST 27
RESTRAINT MOMENT (kip-in)
TOTAL LOAD ON TRUSS ASSEMBLY (lbs)
TENSION STRESS
COMP. STRESS
DEFL.
0
1
2
3
4
5
6
7
8
9
10
0
500
1000
1500
2000
2500
3000
3500
4000

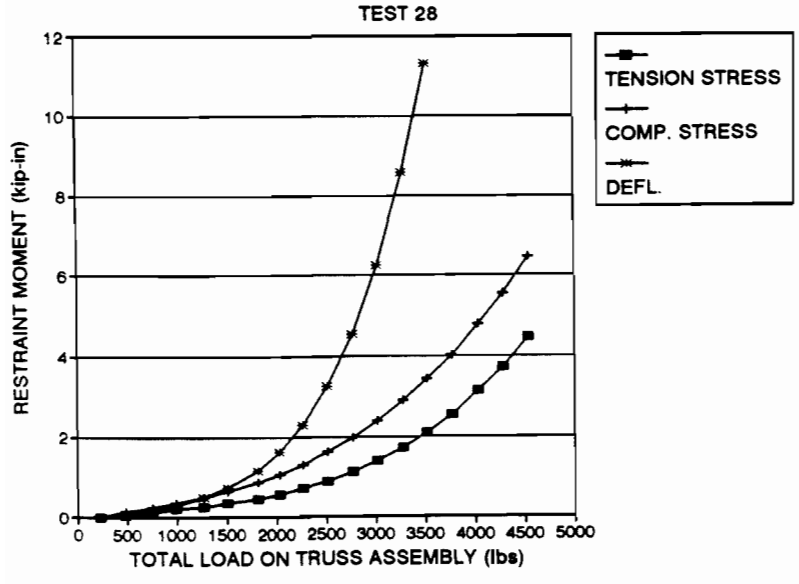
TEST 28
RESTRAINT MOMENT (kip-in)
TOTAL LOAD ON TRUSS ASSEMBLY (lbs)
TENSION STRESS
COMP. STRESS
DEFL.
0
2
4
6
8
10
12
0
500
1000
1500
2000
2500
3000
3500
4000
4500
5000

BIBLIOGRAPHY

1. Haynes, R.W., and Fight, R.D. (1992). Price projections for selected grades of Douglas-fir, coast hem-fir, inland hem-fir, and ponderosa pine lumber. Res. Pap. PNW-RP-447. Portland, OR: U.S. Department of Agriculture, Forest Service, Pacific Northwest Research Station.

2. Harper, M.M., LaBoube, R.A., Yu, W.W. (1995), "Behavior of Cold-Formed Steel Roof Trusses," Summary Report, Civil Engineering Study 95-3, University of Missouri-Rolla.

3. "Specification for the Design of Cold-Formed Steel Structural Members," (1986 with 1989 Addendum). American Iron and Steel Institute.

4. Yu, W.W., (1991). Cold-Formed Steel Design, Second Edition, John Wiley and Sons, Inc., New York.

5. Salmon, C.G. and Johnson, J.E. (1990). Steel Structures: Design and Behavior, Emphasizing Load and Resistance Factor Design, Third Edition, Harper Collins Publishers, Inc., New York.

6. Galambos, T.V. (Ed.). (1988). Guide to Stability Design Criteria for Metal Structures, Fourth Edition, John Wiley and Sons, Inc., New York.

7. "Standard Specifications, Load Tables, and Weight Tables for Steel Joists and Joist Girders." (1994). Steel Joist Institute.

8. Melcher, J.J. (1982). "The Behaviour and the Transverse Deflections Problem of Compression Members," Third International Colloquium on Stability, Timisoara, Romania.

9. "Specifications for Screw Connections," (1993). Center for Cold-Formed Steel Structures Technical Bulletin, Vol. 2, No. 1. American Iron and Steel Institute.

10. Pedreschi, R.F. and Sinha, B.P. (1995). "The Structural Behaviour of Press Joining in Cold-Formed Steel Trusses and Frames," Final Report to Engineering and Physical Sciences Research Council, Research Project GR/H76388, University of Edinburgh.

11. Ife, L.W. (1975). "The Performance of Cold-Formed Steel Products in Housing." Proceedings of the Third International Specialty Conference on Cold-Formed Steel Structures, University of Missouri-Rolla.

12. Woolcock, S.T. and Kitipornchai, S. (1986), "Design of Single Angle Web Struts in Trusses," Journal of Structural Engineering, ASCE, Vol. 112, No.6.

13. "Design Guide for Cold-Formed Steel Trusses," (1995). Publication RG-9518. American Iron and Steel Institute.

14. "Low-Rise Residential Construction Details," (1993). Publication RG-934. American Iron and Steel Institute.